Unbraced pallet rack design in accordance with European practice–Part 1: Selection of the method of analysis

Claudio Bernuzzi [a,*], Armando Gobetti [b], Giammaria Gabbianelli [b], Marco Simoncelli [b]

[a] *Department of Architecture, Built Environment and Construction Engineering, Politecnico di Milano, Milano, Italy*
[b] *Department of Civil Engineering and Architecture, Università di Pavia, Pavia, Italy*

1. Introduction

A very important use of thin-walled cold-formed steel members [1,2] is for the structural systems to store goods and products [3], such as drive-in and drive-through rack systems as well as selective pallet racks. The latter ones, which are considered in the present paper, are spatial framed systems (Fig. 1) composed by a regular sequence of uprights (vertical members) connected to each other. In the down-aisle (longitudinal) direction, beams sustaining pallets (pallet beams) brace uprights and provide adequate stiffness against the down-aisle buckling through semi-rigid connections at the ends of the pallet beams. Furthermore, a significant contribution to the stability is also guaranteed by the connections between the upright bottom ends and the industrial floor (base-plate connections). In the cross-aisle (transversal) direction, bracing members (lacings or diagonals) connect the uprights, forming built-up trussed columns (upright frames).

Racks are quite relatively simple and extremely cheap structures but they are often serviced by sophisticated mechanical handling equipment and could support very expensive goods and products: as a consequence, an eventual their failure should result in a huge economic loss. Generally, when the rack total height is lower than 15–20 m, storage rack systems are usually located inside an independent steel or concrete industrial building, which

* Corresponding author.Tel: +39 0223994246.
E-mail address: claudio.bernuzzi@polimi.it (C. Bernuzzi).

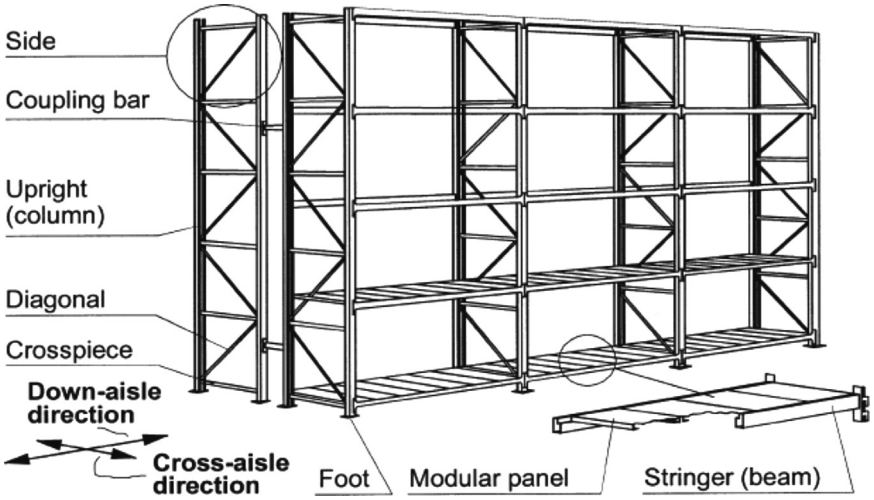

Fig. 1. Typical steel storage pallet rack.

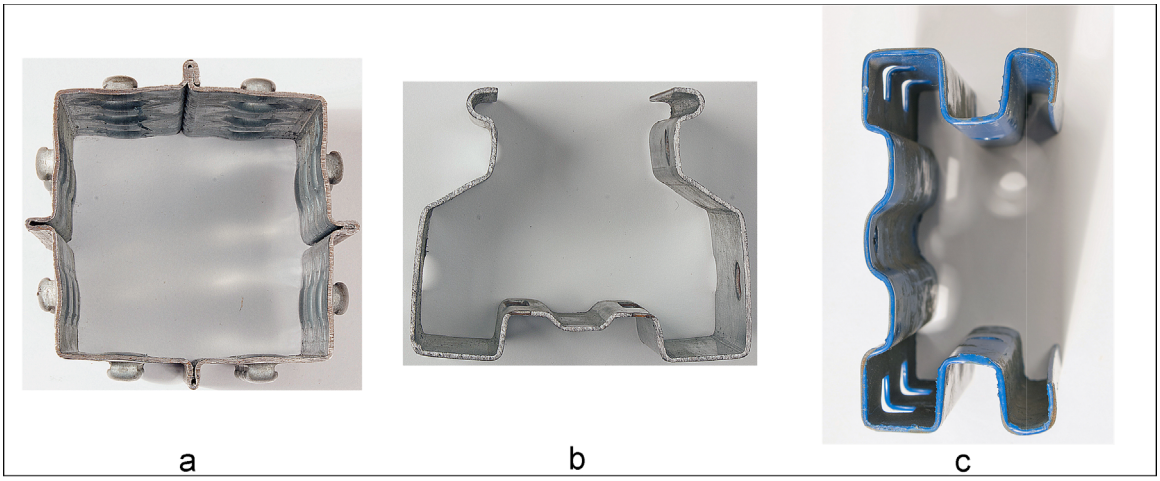

Fig. 2. Typical cross-sections used for uprights (courtesy of Miss Alessandra Pellegatta).

protects them from climatic loads (i.e. wind and snow loads). Increasing the rack height (approximately, up to 50 m [4]), warehouses (i.e. cladding racks) are very conveniently used as storage systems: metal decking sheets are directly connected both to the external upright frames, to form lateral walls, and to the top of upright frames, to form the roof. In general, commercial and marketing reasons prone the manufactures to design the structural key components (mainly, uprights and pallet beams) to minimum weight in order to reduce their cost. Fig. 2 presents some of the typical cross-sections currently used for uprights, which are very similar to the ones considered in the examples of this two-parts paper. Square or rectangular hollow cross-section members are sometimes used in European practice (Fig. 2a) in cases of low- and medium-rise racks but worldwide they are frequently employed in rack warehouse, as well as when racks are located in seismic zones. Otherwise, the cross-sections are quite similar to the lipped channels showed in parts (b) and (c) of the same figure, where the additional rears are used to connect the lacings of the upright frames. Due to the great number of types of beam-end-connectors, as well as to the different geometry of the connected members, theoretical approaches to evaluate the per-formance of members and joints are not currently available [5]. As a consequence, specific tests to quantify main parameters characterizing the response of the key rack components (i.e. pallet beams, uprights, beam-to-column joints and base-plate connections) are required by the most recently revised design standards, [6–9]. On the basis of a suitable re-analysis of tests data, rack design is carried out by using the state-of-the-knowledge devel-oped and codified for traditional thin-walled cold-formed struc-tural systems. As discussed in the following, these rack provisions serve as essential guidelines for practical designers but few further improvements are urgently expected regarding both the structural analysis phase and the stability design rules for members under compression or bending and compression, i.e. for columns and beam-columns, respectively.

Research outcomes presented in this two-parts paper are related to a study in progress in conjunction between the Technical University of Milan and the University of Pavia, which is aimed at improving the design rules for racks. Attention has been focused on medium-rise pallet racks unbraced in the down-aisle direction and subjected to static loads. A parametric analysis has been carried out using an open source finite element program for academic use (Śiva [10]) derived from the original NONSAP [11], to which Authors have added an elasto-plastic spring model and implemented a suitable beam element formulation for mono-symmetric cross-section accounting for warping effects. Six medium-rise rack frames have been selected to give a quite exhaustive overview of racks commonly used in Europe, differing

for the geometry of the whole frame as well as of its components: in particular, three cross-sections were chosen for uprights, having different eccentricity between the shear center and the centroid, which in one case (L_uprights) is null. For each of them a parametric analysis has been carried out by varying the degree of the rotational stiffness of both beam-to-column joints and base-plate connections. Research outcomes are hence presented on the basis of the re-analysis of the data related to 144 rack models.

This initial part of a two-parts papers gives a general overview of the cases considered in the parametric analysis and focuses the attention on the selection of the method of analysis in accordance with the European design approach [6] for steel storage pallet racks. As shown in the following, no clear and univocal rules are provided by the code, and few alternatives, nominally equivalent to each other, are offered to the designers. As a consequence, remarkable differences due to the adopted method of analysis can be observed in the values of internal forces and moments to use for the verification checks, that is the topic discussed in the part 2 ("Essential Verification Checks") of the paper, where the design options admitted by the Code are introduced and directly applied to the same set of racks herein considered.

2. Remarks on the rack structural analysis

Steel storage pallet racks are semi-continuous spatial frames, braced in the cross-aisle direction by built-up laced members forming the upright frames and generally unbraced in the down-aisle direction. As to the structural analysis, the use of finite element (FE) analysis programs offering the semi-rigid joint model is necessarily required to simulate the presence of beam-to-column joints as well as of base-plate connections [12] and particular care should be paid to the joint modeling phase [13]. A very relevant difference from the more traditional steel building structures is due to the use of thin-walled cold-formed members, which are prone to local as well as distortional buckling modes and their direct interactions [14] can reduce significantly rack performances. Furthermore, if open mono-symmetric cross-sections are used, uprights are generally subjected to the flexural–torsional buckling mode, which influences remarkably the overall frame response.

Thin-walled beam theory was well-established by Vlasov [15] and Timoshenko and Gere [16]. For isolated members with mono-symmetric cross-section, outcomes of these studies are nowadays available for structural engineers in terms of equilibrium and compatibility equations governing overall response, prediction of the elastic buckling loads of beams and columns and accurate definition of the complex distribution of normal and tangential stresses over the cross-section. As the reference is made to complete racks, on the basis of authors' experience, it appears that some important key behavioral features are currently neglected, or not adequately considered, in routine design. Structural analysis is usually carried out via FE analysis programs offering only 6 degrees of freedom (DOFs) beam formulations, which have been developed and correctly used for members having two axes of symmetry [17–19], recommended only when the shear center is coincident with the cross-section centroid. For each beam node, 3 displacements (u, v and w) and 3 rotations (φ_x, φ_y, and φ_z) are required (Fig. 3a) to assess accurately the whole set of displacements, internal forces and moments to be used for the verification checks. Very recently, few analysis soft-ware programs allow to include the shear center eccentricity in the set of the cross-section geometrical parameters. Accuracy of results is increased but in the authors' opinion, non-negligible differences can be noted when exact 7DOFs formulation are considered. For this reason, and also considering the limited availability in design office of these 6DOFs improved programs, attention is herein focused on the traditional 6DOFs formulations requiring only 6 geometrical cross-section parameters (area, moments of inertia about principal axes, torsion constant and shear areas). Furthermore, the value of the overall buckling load for sway mode, required to select the method of analysis (i.e. 1st or 2nd order), is consequently determined only on the basis of the flexural buckling modes, that are the ones able to be captured via 6DOFs beam formulations. Design procedures in accordance with major rack codes [6–9] relegate the warping influence only to the flexural–torsional buckling checks of columns and beam-columns, which have to be verified as isolated members of an adequate buckling length. Wagner's constants, warping deformation, shear eccentricity and the coupling between flexure and torsion are neglected in the structural analysis and hence the design procedures currently adopted lead in several cases to incorrect evaluations of the safety level of the racks, as already demonstrated for medium-rise unbraced pallet racks [20,21].

Efficiency of structural engineers has significantly increased, especially in the field of steel structural design, owing to the availability of refined preprocessing software to model quickly very complex steel frames. Furthermore, significant advances in the commercial structural analysis software packages commonly used in designers' offices have been extremely modest over the two decades. Suitable 7DOFs beam formulations accounting for warping effects have already been proposed in literature [10,22–24] and now are implemented in few FE general purpose commercial analysis programs [25–28]. As shown in Fig. 3(b), owing to the eccentricity between the shear center (S) and the centroid (O), in case of FE formulations for mono-symmetric cross-section, reference is made to the shear center for the definition of the whole set of the internal displacements except for the axial displacement u_0, which is related to point O. Shear forces (F_y and F_z), axial force (N) and bi-moment (B) are referred to point S while uniform torsional moment (M_t) and bending moments

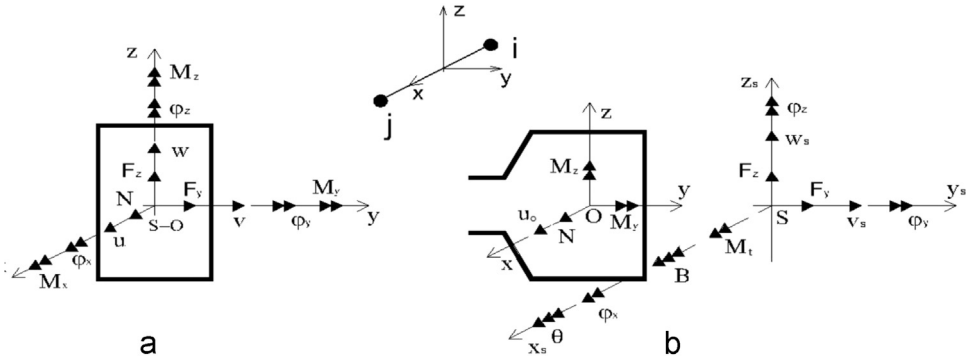

Fig. 3. Set of displacements and internal forces and moments for FE beam formulation with 6DOFs (a) or with 7DOFs per node (b).

(M_y and M_z) are defined with respect to point O. The additional cross-section warping DOF (i.e. the 7th DOF), θ is defined as

$$\theta = \theta(x) = -\frac{d\varphi_x}{dx} \tag{1}$$

Only the presence of warping θ is an essential pre-requisite to guarantee that rack design is carried out considering adequately key features of mono-symmetric cross-section members: the presence of warping can be found in the torsional coefficients of the elastic beam stiffness matrix $[K]_j^E$, as briefly shown in Appendix A. From a practical point of view, in addition to the presence of bi-moment (B) and a different value of the torsional moment (M_t), a relevant influence of warping is expected also in the value of the bending moments and consequently, in the shear forces. In correspondence of the nodal points, rack members (uprights, pallet beams and lacings) are in fact connected to each other and their cross-sections are characterized by different relative positions of the centroids and of the shear centers. As a consequence, the complex mutual interactions of the transferred end member forces, governed by the traditional equilibrium and compatibility principles, lead to significant differences of internal forces and moments, when compared with the ones associated with the commonly adopted 6DOFs beam formulations. Furthermore, if a 2nd elastic order analysis has to be adopted, as generally occurs in routine rack design,a traditional 6DOFs beam formulation requires the knowledge of the sole value of the internal axial load N, despite the fact that this procedure should not be totally correct also with reference to frames made by bi-symmetric cross-section members, as discussed in the following. Otherwise, in case of beam formulations including warping, also the values of the bending moments (M_y and M_z), torsional moment (M_t), bi-moment (B) and shear actions (F_y and F_z) contribute significantly to form the geometric stiffness $[K]^G$. The terms of $[K]^G$ depend strictly also on the distance between the load application point and the shear center, as well as on all the Wagner's coefficients. Only the presence of the 7th DOF makes possible to estimate correctly both frame displacements and internal forces and moments, which govern the local state of stresses of each upright cross-section. Furthermore, as previously observed, these formulations are the only able to capture directly also the overall flexural–torsional buckling phenomena of the frame, avoiding hence the complex and not univocal definition of the appropriate effective length of isolated members, which is required by the procedure currently adopted for rack design. As a general comment, it should be noted that the diffusion among rack designers of the available commercial analysis software programs offering 7DOFs FE beam element formulations is nowadays extremely limited. Main reasons for this should be the difficulties associated with the correct use of them, the high engineering competences required and the very limited possibilities to model directly complex cross-section geometries similar to the ones presented in Fig. 2.

As previously mentioned, the European rack design is currently carried out in accordance with the EN 15512 provisions [6]. The set of displacements and internal forces and moments are evaluated by means of a 1st or 2nd order elastic analysis, depending on the stability to lateral loads. From a practical point of view, this very important choice depends on the value of the critical load multiplier α_{cr}, defined as the ratio between the elastic critical buckling load for global instability mode (V_{cr}) and the total design vertical load of the structure (V_{Ed}), i.e. $\alpha_{cr}=V_{cr}/V_{Ed}$. In particular, as reported also in the Australian rack code [9], it is recommended that, if $\alpha_{cr} \geq 10$ (or, equivalently, if $V_{Ed}/V_{cr} \leq 0.1$), the rack has to be treated as non-sway frame and a 1st order analysis is considered adequate to design purposes. Otherwise, if $\alpha_{cr} \leq 10$ (or, equivalently, if $V_{Ed}/V_{cr} \geq 0.1$), the rack is a sway frame and 2nd order effects have to be directly considered into structural analysis. It should be noted that, if $3.33 \leq \alpha_{cr} \leq 10$ (or, equivalently, if $0.1 \leq V_{Ed}/V_{cr} \leq 0.3$), the 2nd order effects could also be treated indirectly, via simplified approaches, such as the *Amplified Sway Moment Method* [29].

When uprights are made from mono-symmetric cross-section, suitable 7DOFs FE beam formulations have to take necessarily and adequately into account key features of the constituent rack members. Otherwise, as shown in Appendix A, if Wagner's constants, warping torsion and shear center eccentricity are neglected for open mono-symmetric cross-section members, design is inevitably affected by methodical errors: from the selection of the analysis method to the assessment of the normal and tangential internal stresses, including, of course, the evaluation of design internal forces and moments and of the set of displacements. These very important aspects are currently ignored by standard codes: no minimum requirements are at present clearly specified for the accuracy of the FE formulations nor reference is made to any benchmark to check of the adequacy of the FE analysis programs to model racks. Direct consequences are that designers (1) use commercial software packages offering only 6DOFs beam formulations (the centroid is often coincident with the shear center) also to model mono-symmetric cross-section members and (2) believe that the design is characterized by a more than adequate level of safety because it meets all the standard requirements. As clearly stated by Bernuzzi et al. [20,21],influence of warping effects on design is of paramount importance: neglecting warping effects, elastic critical overall load multiplier is significantly overestimated. Furthermore, also internal forces and bending moments are significantly influenced by the FE beam formulation adopted in structural analysis and hence not negligible differences are expected with reference to the different options which designers could adopt for the serviceability, resistance and stability verification checks.

3. The considered racks

As previously mentioned, racks are regular structural systems and in the present paper attention has been focused on three

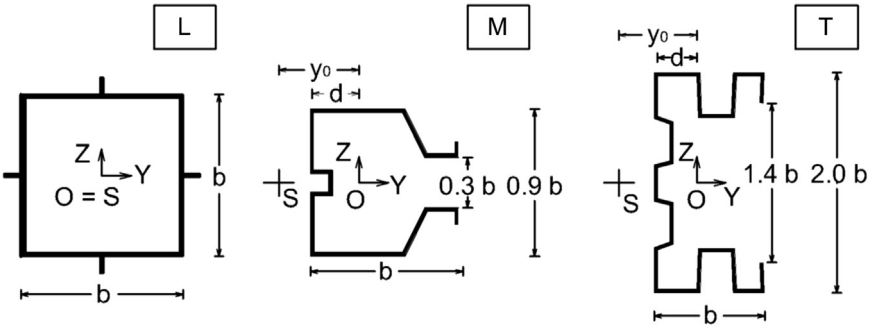

Fig. 4. Cross-sections considered in the present study.

rack types (identified in the following as *L*, *M* and *T*) differing for the upright cross-section geometries, which have been selected (Fig. 4) to be representative for uprights typically employed for medium-rise racks, unbraced in the down-aisle direction. In particular:

- the hollow cross-section *L* (Fig. 2a) presents two axes of symmetry, and the closure of this square cross-section is obtained by overlapping and clamping to each other the lateral edges of the strip coils at the middle of one of the four sides. The clamped zone and the zones in correspondence of the intermediate stiffener on the middle of the three other faces contribute to reduce significantly the weakening effects due to local buckling;
- the open mono-symmetric cross-section *M* is similar to a lipped channel with additional rears to bolt the upright lacings. This upright, which is one of the most commonly used by several European manufactures, is characterized by an internal stiffener of the plate (web) restrained by the flanges in order to reduce local buckling effects;
- the open mono-symmetric cross-section *T* presents one axis of symmetry but differs from the M_ type because of the presence of two internal stiffeners on the web and one internal stiffener on each flange, which is used to bolt directly the upright lacings.

Table 1
Key data of the considered cross-section uprights.

Section properties	L	M	T
I_y/I_z	1.000	0.992	4.709
ρ_y/ρ_z	1.000	0.996	2.170
$W_y/W_{z,sup}$	1.000	1.233	2.990
$W_y/W_{z,inf}$	1.000	0.838	1.793
y_0/d	0.000	2.306	1.989
I_t [mm^4]	0.985×10^6	0.619×10^3	0.972×10^3
I_w [mm^6]	0.178×10^6	1.600×10^9	0.630×10^9
ω_{max} [mm^2]	–	3.249×10^3	1.578×10^3

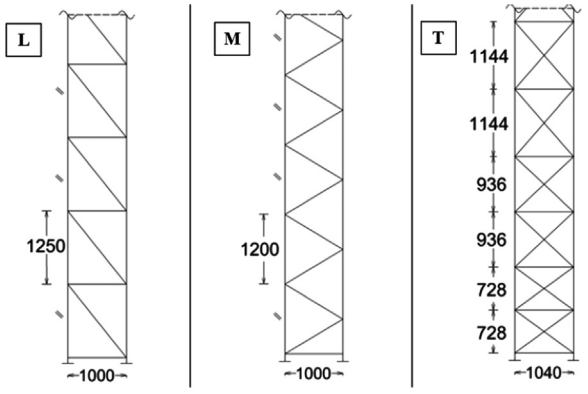

Fig. 5. Upright frames for L_racks (a), M_racks (b), and T_racks (c).

For each of these uprights cross-section, the ratios between second moment of area (I_y/I_z), section moduli ($W_y/W_{z,inf}$ and $W_y/W_{z,sup}$) and ratio between radius of gyration (ρ_y/ρ_z) are reported in Table 1, together with the non-dimensional eccentricity y_0/d, i.e. the eccentricity (y_0) between the shear center and the centroid over the distance between the centroid and the web (d). Furthermore, the uniform torsional and warping second moment of area (I_t and I_w, respectively) and the maximum value of the first moment of the sectorial area (ω_{max}) are reported in the table, too. No additional data such as the complete geometries of the cross-section have been possible to present directly in the paper because of the confidentiality required from manufactures on their patented products considered in the present study. These selected upright cross-sections present significant differences in geometric properties, as it appears by considering the value of I_y/I_z (ranging from 1.0 to 4.7) and y_0/d (from 0.0 to 2.3) and this authors' choice is to allow a quite exhaustive overview of the cases most frequently encountered in routine rack design.

Reference has been made to pallet racks unbraced in the down-aisle direction with six equal bays; the depth of the upright frame was assumed equal to 1.00 m for L_ and M_racks and to 1.04 m for T_racks. A single upright frame geometry (Fig. 5) and two configurations in the down-aisle direction, differing for the number of load levels (N_{LL}) have been associated with each upright. In case of L_ and M_racks, transversal stability is provided by typical *Z*- and *V*-upright panels while for T_racks, the more traditional X-cross brace panels guarantee stability to the cross-aisle loads. Table 2 represents the key data of the racks considered in the numerical analysis in terms of pallet beam span (L_b), interstorey height (h_{LL}), total height (H_{tot}) and number of load levels (N_{LL}). Other key data are presented in the same table, which reports also the height of the upright panel frame (h_u) in correspondence of the first load level. Pallet beams are realized by means of rectangular hollow sections (*RHS*); as to the lacings of the upright frames, square hollow sections (*SHS*) have been used for M_ and G_racks while, for T_racks, circular hollow sections (*CHS*) resisting both to tension and compression have been used. All the rack components belong to class 3 of Eurocode 3 [29], i.e. they are characterized by the absence of post-elastic resources. As to the load conditions, the sole case of fully loaded racks was considered with pallet units acting as uniform load on pallet beams. An overall frame imperfection equal to 0.0033 rad (1/300 rad) in terms of out-of-plumb of the uprights in both the cross- and down-aisle directions has been considered simulta-neously, simulated via horizontal forces concentrated on each floor level. Attention has been focused on the following parameters:

- the degree of flexural stiffness associated with beam-to-column joints. The selection of the values of the elastic rotational stiffness of beam-to-column joints, $S_{j,btc}$ was based on the

Table 2
Key data of the considered medium-rise rack frames.

Racks	Down-aisle direction					Cross-aisle direction		
	L_b [m]	Beam pallets section	h_{LL} [m]	H_{tot} [m]	N_{LL}	Type of brace	Upriget type	h_u [m]
L_3	2.78	RHS $100 \times 50 \times 3.0$ mm	2.25	7.60	3	SHS $30 \times 30 \times 3$ mm	L	1.25
L_5	2.78		1.50	7.60	5			1.25
M_4	2.78	RHS $100 \times 40 \times 1.3$ mm	1.80	7.20	4	SHS $30 \times 30 \times 3$ mm	M	1.20
M_5	2.78		1.20	6.30	5			1.20
T_3	2.83	RHS $165 \times 40 \times 2.0$ mm	2.50	8.25	3	CHS $d=30$ mm $t=1.5$ mm	T	0.92
T_4	2.83		1.97	8.25	4			0.73

classification criteria of part 1–8 of EC3 [30]. In particular, few values of $S_{j,btc}$ of interest for practical application [13], have been expressed as multiple (by means of term $\rho_{j,btc}$) of a reference stiffness value $S_{j,btc}^{EC3-LB}$ via the relation:

$$S_{j,btc} = \rho_{j,btc} \cdot S_{j,btc}^{EC3-LB} \tag{2a}$$

where $S_{j,btc}^{EC3-LB}$ is the rotational stiffness associated with the lower bound of the semi-rigid domain, i.e. the value corresponding to the transition between the regions of flexible (pinned) and semi-rigid joints, which is defined as

$$S_{j,btc}^{EC3-LB} = 0.5\frac{EI_b}{L_b} \tag{2b}$$

where E is the Young's modulus, I_b the second moment of area and L_b the length of the beam.

Parameter $\rho_{j,btc}$ has been assumed ranging from 0.5 to 10. Lowest values are typically obtained from tests on boltless connections, the greatest ones correspond to the same connection types but strengthened via one M10 or M12 bolt connecting the beam end bracket to the upright face to increase the joint performance, especially in seismic zones, in terms of stiffness and ductility. The considered values of the joint stiffness are presented in Fig. 6 in the non-dimensional $\overline{m} - \overline{\phi}$ domain, being $\overline{m}$ and $\overline{\phi}$ defined as

$$\overline{m} = \frac{M}{M_{pl,Rd}} \tag{3a}$$

$$\overline{\phi} = \phi\frac{EI_b}{L_b M_{pl,Rd}} = \phi\frac{S_{j,btc}}{2 \cdot \rho_{j,btc} M_{pl,Rd}} \tag{3b}$$

where M and ϕ are respectively the moment and the rotation of the joint (with the elastic stiffness directly defined as $S_{j,btc} = M/\phi$) and $M_{pl,Rd}$ is the plastic moment of the beam.

- the degree of flexural stiffness associated with the base-plate connections. As stated in [30], the rotational stiffness $S_{j,base}^{EC3-UB}$ at the boundary between the regions of semi-rigid and rigid base-plate joints is assumed equal to

$$S_{j,base}^{EC3-UB} = 30\frac{EI_u}{h_{LL}} \tag{4}$$

where I_u is the second moment of area of the upright cross-section and h_{LL} is the system length from the foundation to the first load level in the down-aisle direction.

As for beam-to-column joints, the base-plate connection restraint has been also parametrically defined: the values of the rotational stiffness $S_{j,base}$ have been selected as multiple, by means of term $\rho_{j,base}$, of the upper transition stiffness defined as

$$S_{j,base} = \rho_{j,base} \cdot S_{j,base}^{EC3-UB} \tag{5}$$

Three values have been considered ($\rho_{j,base}$=0.15, $\rho_{j,base}$=0.30 and $\rho_{j,base}$=0.45) to characterize the base-plate connections,

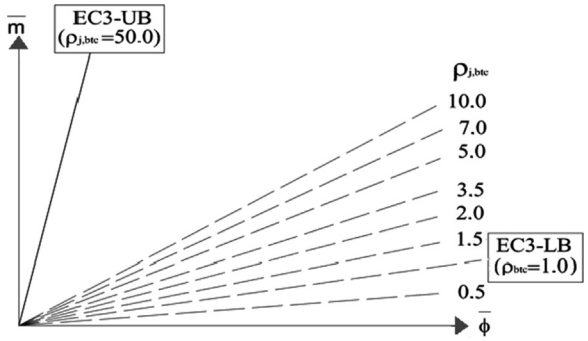

Fig. 6. Considered values of the rotational stiffness for beam-to-column joints.

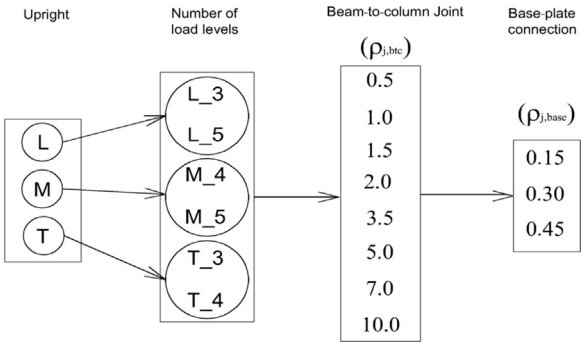

Fig. 7. Synopsis of the cases considered in the parametric analysis.

despite several studies on similar topics have in the past assumed the ideal restraints of hinged and fixed basis [20,31].

The considered racks have been analyzed by using both 6DOFs and 7DOFs beam element formulations, both offered by Śiva software [10], and Fig. 7 presents the layout of the executed analysis explaining the symbols used to present research outcomes. In accordance with European practice, the thick brackets are welded to the beam ends and the lacings are bolted in the oversized holes in the upright flanges. For this reason, warping restraint has been considered free for the upright top and for the lacings; at the beam ends, due to the types of beam end connectors commonly used for the considered racks, warping was blocked as well as at the bottom of the uprights.

4. Method of analysis to assess the overall rack response

There are no clear requirements in the European rack code on the key features associated with the evaluation of the elastic critical load multiplier. Buckling analysis is recommended without any indication on the acceptability of the computer results nor on the minimum requirements for the evaluation of the adequacy of the FE beam formulation. As a general remark it should be noted that special care should be paid to the interpretation of the buckling analysis results and, as an example, the upright frame of Fig. 8 can be considered, where the *X*-bracing systems are composed by diagonal members resisting only to tension (a). Due to lack of a mono-lateral truss element resisting only to tension (i.e. rope element), in the most common FE commercial software packages a bi-lateral truss element (resisting both to tension and compression) is usually adopted by designers to model the diagonals: reference is hence made to the model in Fig. 8(b). Critical load multipliers associated with deformed shapes similar to the ones in parts (c) and (d) could be obtained, out of range of validity and interest for design purposes: when the compressed diagonals buckle the structure is however safe because of the resistance of the tension diagonals, despite the buckling of one component. As a consequence, the sole buckling deformed shape of interest for practical design purposes is the one presented in part (e) of the figure, related to an overall buckling mode.

Very frequently, designers use 6DOFs FE beam formulations and the choice of the analysis method depends on the value of the sole flexural buckling critical load multiplier α_{cr}^{6}. If reference is made to commercial FE analysis software programs, the formula-tion adopted to evaluate 2nd order effects and to execute linear buckling analyses require the knowledge [18,32] of the sole value of internal axial forces on members (N), which contributes to define the terms of the geometric stiffness matrix $[K]^G$. From a theoretical point of view it is worth to mention that also bending moments contribute to define $[K]^G$, as clearly shown also in

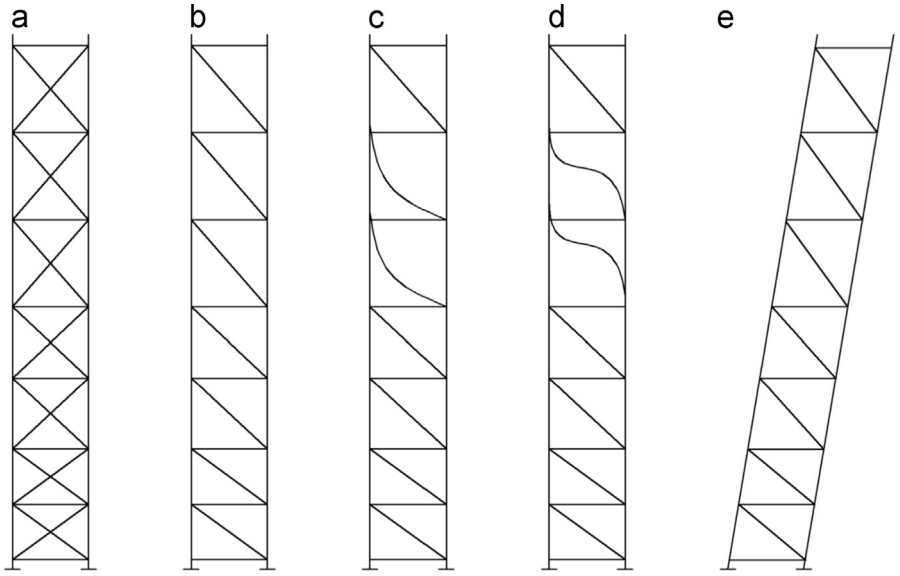

Fig. 8. T_upright X-braced frames with diagonal resisting only to tension (a): model for FE analysis with truss elements as diagonals (b), typical buckling shapes out of interest (c and d) and example of a buckling shape of interest for design purpose (e).

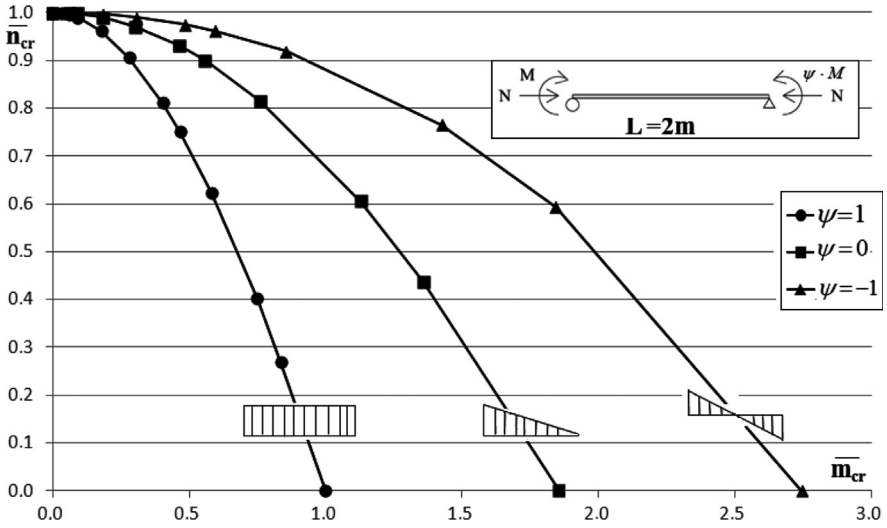

Fig. 9. Example of elastic critical non-dimensional mcr ncr domain for an isolated, simply supported beam-column subjected to constant or gradient moments.

Refs. [33–35], where computer structural analysis and design of traditional steel frames, i.e. made by bi-symmetric cross-section members are discussed. Furthermore, when thin-walled open cross-sections are used, as clearly demonstrated by Teh et al. [36] with reference to a double-side high-rise steel pallet rack, the buckling load factor evaluated via FE commercial analysis programs should not be adequate for design purpose. As an example of the effect of the interaction between the axial load and the bending moment on buckling conditions, Fig. 9 can be considered. The elastic critical domains obtained by Śiva software are presented for the M_uprigths: an isolated simply supported member axially loaded at its ends and subjected to constant ($\psi=1$) or gradient ($\psi=0$ and $\psi=-1$) moments has been modeled by varying the ratio between axial load (N), and bending moment (M). Data are presented in the non-dimensional domain $\overline{n_{cr}}-\overline{m_{cr}}$: the critical axial load (N_{cr}) has been divided by the critical value associated with pure compression, i.e. $\overline{n_{cr}}=N_{cr}/N_{cr}(M_{cr}=0)$, and the critical bending moment (M_{cr}) by the critical bending moment associated with pure flexure in case of uniform moment distribution ($\psi=1$), i.e. $\overline{m_{cr}}=M_{cr}/M_{cr}(N_{cr}=0,\psi=1)$.

The influence on the critical axial load on the bending moment distribution along the member can be noted, as it appears also by the associated deformed shapes obtained from an elastic buckling analysis, and represented, as an example, in Fig. 10. If the presence of bending moments in the geometric stiffness matrix $[K]^G$ is neglected, it is assumed that the critical load conditions of the beam-column are governed by the sole value of the axial load, leading this assumption to a non-negligible overestimation of the buckling resistance, also for low values of the applied bending moment. Formulations of $[K]^G$ requiring the sole value of the axial load acting on member should be hence a source of potential errors for buckling as well as for structural analysis. With the aim of investigating this aspect, L_racks were analyzed in the present study using, in addition to the 6DOFs beam formulation, the 7DOFs one, whose geometric stiffness matrix contains also the bending moment contribution, as shown in Appendix A.

As previously discussed, most commonly used FE analysis programs are inadequate to design mono-symmetric uprights mainly because they neglect the very important warping effects. It is hence clear that, in these cases, the use of 7DOFs beam

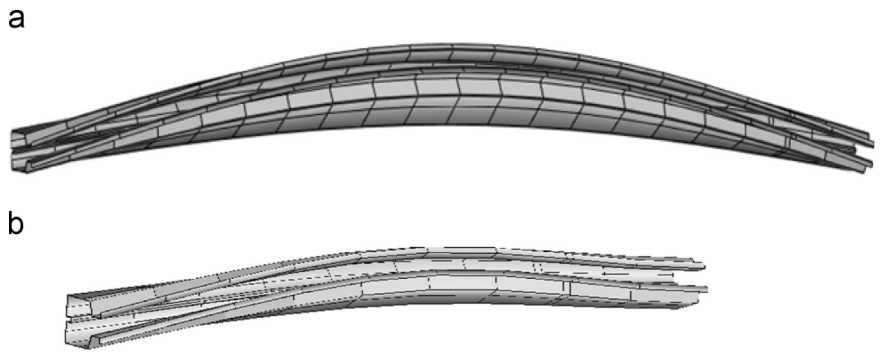

Fig. 10. Buckling deformed shapes of an isolated simply supported beam-column subjected to uniform moment, ($\psi = 1$): M_ upright with two different length, (a) $L=2000$ mm and (b) $L=1000$ mm.

element formulations is strongly recommended, which leads to obtain the "exact" value of the critical elastic load multiplier or the associated multiplier, identified in the following as α_{cr}^{7}.

Furthermore, also the approximated methods admitted by rack codes [6,9] to estimate the critical load conditions should be a potential source of errors if warping is neglected. In particular, the well-known Horne's method [37], is currently recommended to predict V_{cr}, or α_{cr}, respectively as

$$V_{cr} = \frac{\phi}{\phi_{max}} V_{Ed} \tag{7a}$$

$$\alpha_{cr} = \frac{\phi}{\phi_{max}} \tag{7b}$$

where ϕ is the frame imperfection defined as an equal out-of-plumb of all the uprights of the racks and ϕ_{max} is the largest value of the sway index ϕ_s of any storey (interstorey drift), defined as

$$\phi_s = (\delta_u - \delta_L)/h_{LL} \tag{8}$$

where h_{LL} is the storey height and δ_u and δ_L are the horizontal deflection at the top and at the bottom of the storey, respectively.

Owing to the importance and to the diffusion of this simplified approach, its accuracy has been evaluated on the set of racks already introduced in Section 3.1.

4.1. Numerical applications

The elastic critical load multipliers associated with the 6DOFs and 7DOFs FE beam formulations of Śiva have been at first directly evaluated for each rack via a buckling analysis, identified in the following as α_{cr}^{6} and α_{cr}^{7}, respectively. To allow a direct appraisal of the warping effects on the structural analysis results, Fig. 11 shows two typical deformed shapes obtained by a buckling analysis with 6DOFs (a) and 7DOFs (b) FE beam formulation. Reference is made to the M_4 rack with $\rho_{j,btc}=0.50$: its deformed shape in Fig. 11(a) is governed by the flexural buckling of the uprights (6DOFs); otherwise if 7DOFs beam formulation results are considered, the coupling with flexure and torsion can be appraised directly in each part of the uprights delimited by pallet beams and/or lacings, via the relevant rotation of the cross-sections.

In order to single out the warping influence on the overall buckling frame response, reference can be made to the ratios $\alpha_{cr}^{6}/\alpha_{cr}^{7}$ presented in Tables 3 and 4 for all the considered racks. The former is related to racks made by bi-symmetric cross-section members (L_racks) and the latter is for the cases of racks made by mono-symmetric profiles (M_ and T_racks).

If L_racks are considered, very negligible differences should be expected between α_{cr}^{6} and α_{cr}^{7}, because of the absence of the warping effects, being the centroid coincident with the shear center. From Table 3 it can be noted that ratio $\alpha_{cr}^{6}/\alpha_{cr}^{7}$ is approximately the unity, with differences extremely limited (never greater than 1%) due to the bending moment distributions, i.e. to the presence of terms influenced by the bending moment value in the geometric stiffness matrix associated with 7DOFs FE buckling analysis. As a conclusion, the actual moment distributions in the buckling analyses can be neglected without excessive approximations of the critical load conditions despite the interaction between N_{cr} and M_{cr} (Fig. 9).

Table 4 is related to M_ and T_racks; it can be noted that:

- increasing the degree of the rotational stiffness of the beam-to-column joints, the ratio $\alpha_{cr}^{6}/\alpha_{cr}^{7}$ increases too, up to 1.16, underlining the importance of warping effects for open cross-sections;
- for T_3 and T_4 racks this influence is slightly lower and the overestimation of the buckling load multiplier obtained with 6DOFs beam formulation is never greater than 7%, due to the quite reduced importance of the coupling between flexural and torsional buckling for this type of upright;
- the ratio $\alpha_{cr}^{6}/\alpha_{cr}^{7}$ for M_ and T_racks is quite influenced by the stiffness of base-plate connections: increasing $\rho_{j,base}$, term $\alpha_{cr}^{6}/\alpha_{cr}^{7}$ increases moderately, especially for higher values of $\rho_{j,btc}$;
- the lowest values of the errors are associated with the lowest value of $\rho_{j,btc}$ and increasing the stiffness of base-plate connections, the errors increase, too; furthermore it is possible to observe the quite limited dispersion of the data related to the T_racks.

Finally, it should be remarked that, as previously observed for L_racks, the differences in the prediction of the "exact" critical load multiplier (identified in this study as the one obtained from the 7DOFs analysis α_{cr}^{7}) via a 6DOFs buckling analysis are completely due to the warping influence, being the effects of the bending moment distributions on the overall rack buckling negligible for practical design purposes.

Both the set of horizontal displacements obtained via a 1st order elastic analysis based on 6DOFs and 7DOFs beam element formulations have been used to predict the associated elastic critical load multipliers via Horne's method, which are in the following identified as ${\alpha^{6}}_{cr}{}^{-H}$ and ${\alpha^{7}}_{cr}{}^{-H}$, respectively. In Tables 3 and 4, the ratios ${\alpha^{6}}_{cr}{}^{-H}/{\alpha^{7}}_{cr}$ and ${\alpha^{7}}_{cr}{}^{-H}/{\alpha^{7}}_{cr}$ allow a direct appraisal of the accuracy of this simplified approach as well as to quantify the errors associated when warping is neglected in this prediction method. With reference to racks made by bi-symmetric cross-section members (Table 3) terms ${\alpha^{6}}_{cr}{}^{-H}$ and ${\alpha^{7}}_{cr}{}^{-H}$ are practically coincident, as clearly expected for the previously discussed reasons. Moreover, the prediction with Horne's method is generally from

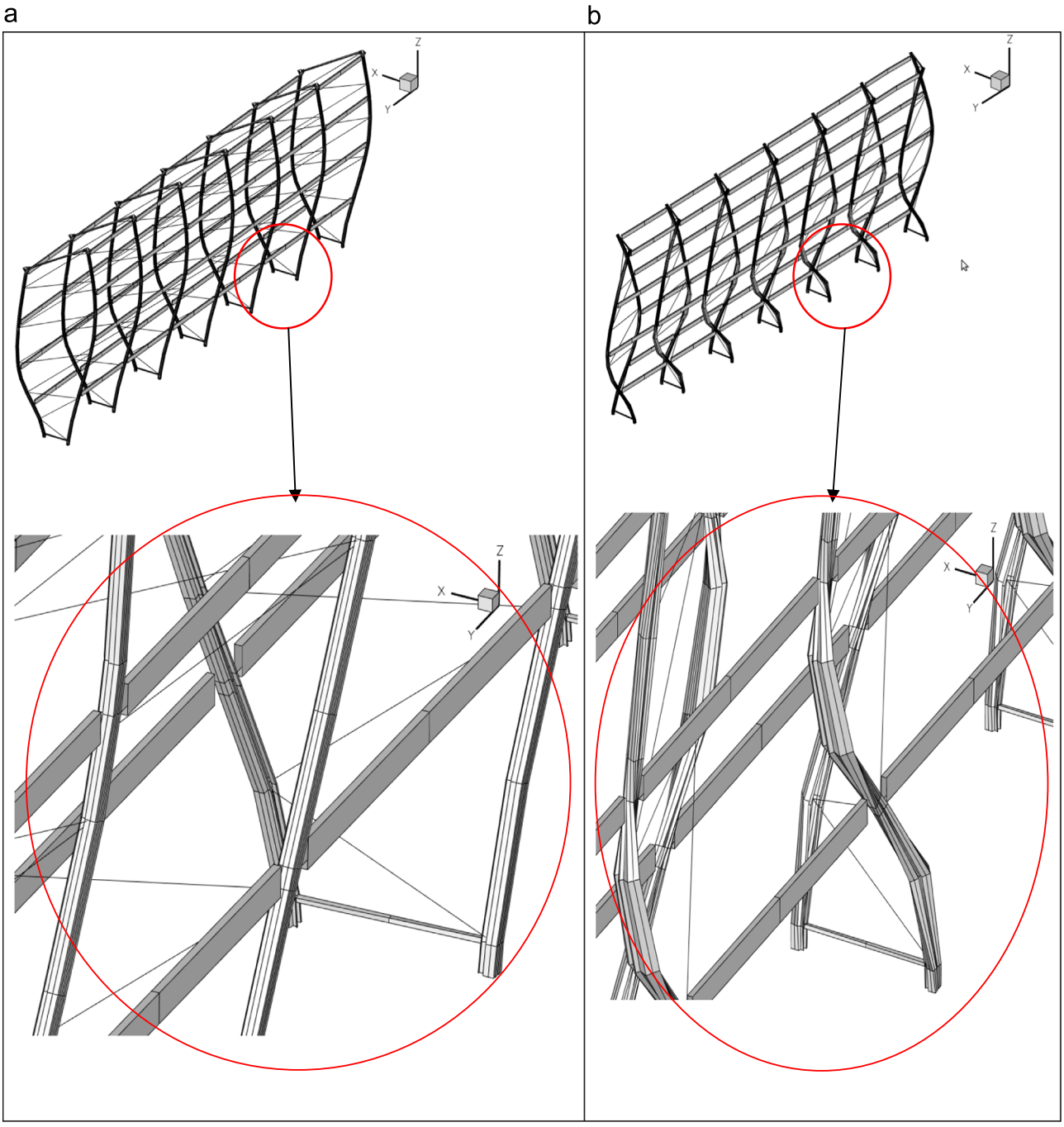

Fig. 11. Comparison between the overall buckling deformed shape obtained via a 6DOFs (a) and 7DOFs (b) FE buckling analysis.

the safe side, except than for two cases related to L_3 racks (i.e. $\rho_{j,btc}=7.0$ with $\rho_{j,base}=0.30$ and $\rho_{j,btc}=10.0$ with $\rho_{j,base}=0.45$), to which correspond a very moderate overestimation of the buckling load (in any case lower than 3%). Maximum errors, however never greater than 13%, are associated with the lower value of $\rho_{j,btc}$; increasing the beam-to-column joint stiffness, the error decreases up to 4%. It can be noted that for L_5 racks, i.e. the ones with the lower value of the interstorey level, ratio $\alpha_{cr}^{6-H}/\alpha_{cr}^{7}$ is quite constant up to $\rho_{j,btc}=0.3$ approximately, and then it increases moderately. Otherwise, the errors associated with the L_3 racks decrease significantly also for the lower values of $\rho_{j,btc}$.

Further comments arise from data of Table 4, i.e. the one associated with M_ and T_racks to better appraise the influence of warping effects on the Horne's method. It appears that the use of the 6DOFs FE set of displacements in case of very flexible racks, i.e. with the lowest values of $\rho_{j,btc}$ and $\rho_{j,base}$, leads to a moderate underestimation of α_{cr}^{7}, up to 13%, as for L_racks. Otherwise, the elastic critical load multiplier is significantly overestimated: up to 11% for M_racks and in case of T_3 racks up to 9%, owing to the more limited influence of the warping on the cross-section geometry.

It can be noted that warping effects lead to values of Horne's multiplier slightly lower than the corresponding one obtained via 6DOFs displacements: as a consequence, the non-negligible overestimation previously mentioned is reduced for high value of $\rho_{j,btc}$. The ratio $\alpha_{cr}^{7-H}/\alpha_{cr}^{7}$ is generally lower than unity, up to 0.84, with a very limited number of exceptions, but however this ratio is never greater than 1.04, confirming that this simplified approach should be of interest for practical design, when warping is adequately considered.

Table 3
Overall buckling load multiplier for bi-symmetric cross-section uprights: influence of the moment distribution on the upright ($\alpha_{cr}^{6}/\alpha_{cr}^{7}$) and accuracy of the Horne's approach ($\alpha_{cr}^{6-H}/\alpha_{cr}^{7}$ and $\alpha_{cr}^{7-H}/\alpha_{cr}^{7}$).

Racks	$\rho_{j,btc}$	$\rho_{j,base}=0.15$			$\rho_{j,base}=0.30$			$\rho_{j,base}=0.45$		
		$\alpha_{cr}^{6}/\alpha_{cr}^{7}$	$\alpha_{cr}^{6-H}/\alpha_{cr}^{7}$	$\alpha_{cr}^{7-H}/\alpha_{cr}^{7}$	$\alpha_{cr}^{6}/\alpha_{cr}^{7}$	$\alpha_{cr}^{6-H}/\alpha_{cr}^{7}$	$\alpha_{cr}^{7-H}/\alpha_{cr}^{7}$	$\alpha_{cr}^{6}/\alpha_{cr}^{7}$	$\alpha_{cr}^{6-H}/\alpha_{cr}^{7}$	$\alpha_{cr}^{7-H}/\alpha_{cr}^{7}$
L_3	0.5	0.999	0.884	0.883	1.002	0.884	0.882	1.002	0.884	0.882
	1.0	0.999	0.890	0.889	1.001	0.879	0.878	0.998	0.879	0.877
	1.5	1.000	0.907	0.906	1.001	0.888	0.886	1.004	0.884	0.883
	2.0	1.001	0.924	0.926	0.995	0.896	0.897	1.001	0.891	0.890
	3.5	1.002	0.986	0.985	1.002	0.939	0.939	1.001	0.927	0.924
	5.0	1.002	0.976	0.975	1.003	0.975	0.975	1.002	0.956	0.955
	7.0	1.002	0.965	0.965	1.001	1.012	1.012	1.001	0.990	0.990
	10.0	1.001	0.959	0.960	1.003	1.000	1.000	1.003	1.026	1.026
L_5	0.5	1.000	0.875	0.871	1.009	0.878	0.874	1.009	0.872	0.868
	1.0	1.002	0.886	0.884	1.002	0.890	0.886	1.004	0.887	0.883
	1.5	0.999	0.872	0.871	1.000	0.876	0.874	0.999	0.880	0.875
	2.0	1.001	0.873	0.872	1.002	0.871	0.870	0.999	0.870	0.869
	3.5	0.999	0.885	0.885	1.001	0.873	0.872	0.997	0.872	0.870
	5.0	0.998	0.905	0.903	0.999	0.887	0.885	1.000	0.880	0.880
	7.0	0.998	0.931	0.929	0.997	0.902	0.900	0.999	0.894	0.894
	10.0	1.000	0.960	0.961	0.999	0.924	0.923	0.998	0.914	0.912

Table 4
Overall buckling load multiplier for mono-symmetric cross-section uprights: influence of the warping ($\alpha_{cr}^{6}/\alpha_{cr}^{7}$) and accuracy of Horne's method neglecting ($\alpha_{cr}^{6-H}/\alpha_{cr}^{7}$) or considering warping ($\alpha_{cr}^{7-H}/\alpha_{cr}^{7}$).

Racks	$\rho_{j,btc}$	$\rho_{j,base}=0.15$			$\rho_{j,base}=0.30$			$\rho_{j,base}=0.45$		
		$\alpha_{cr}^{6}/\alpha_{cr}^{7}$	$\alpha_{cr}^{6-H}/\alpha_{cr}^{7}$	$\alpha_{cr}^{7-H}/\alpha_{cr}^{7}$	$\alpha_{cr}^{6}/\alpha_{cr}^{7}$	$\alpha_{cr}^{6-H}/\alpha_{cr}^{7}$	$\alpha_{cr}^{7-H}/\alpha_{cr}^{7}$	$\alpha_{cr}^{6}/\alpha_{cr}^{7}$	$\alpha_{cr}^{6-H}/\alpha_{cr}^{7}$	$\alpha_{cr}^{7-H}/\alpha_{cr}^{7}$
M_4	0.5	1.010	0.881	0.868	1.019	0.885	0.867	1.012	0.878	0.866
	1.0	1.028	0.918	0.885	1.030	0.902	0.872	1.038	0.899	0.869
	1.5	1.041	0.961	0.908	1.046	0.934	0.888	1.045	0.926	0.881
	2.0	1.053	1.006	0.938	1.053	0.967	0.904	1.061	0.960	0.898
	3.5	1.063	1.025	0.969	1.073	1.051	0.948	1.081	1.037	0.936
	5.0	1.065	1.021	0.956	1.082	1.083	0.981	1.093	1.095	0.963
	7.0	1.065	1.021	0.949	1.089	1.076	1.001	1.101	1.114	0.992
	10.0	1.071	1.026	0.945	1.092	1.076	0.992	1.104	1.111	1.022
M_5	0.5	1.005	0.889	0.881	1.010	0.897	0.880	1.005	0.894	0.874
	1.0	1.025	0.896	0.871	1.027	0.916	0.872	1.030	0.901	0.873
	1.5	1.040	0.934	0.881	1.047	0.926	0.876	1.049	0.924	0.876
	2.0	1.053	0.951	0.895	1.060	0.954	0.883	1.064	0.950	0.881
	3.5	1.078	1.013	0.934	1.094	1.037	0.914	1.100	1.030	0.909
	5.0	1.092	0.993	0.968	1.115	1.090	0.938	1.122	1.096	0.931
	7.0	1.099	0.981	0.962	1.130	1.062	0.964	1.142	1.108	0.956
	10.0	1.103	1.031	0.947	1.143	1.053	0.991	1.159	1.094	0.980
T_3	0.5	1.024	0.906	0.879	1.034	0.901	0.870	1.030	0.900	0.868
	1.0	1.028	0.948	0.918	1.032	0.925	0.892	1.034	0.919	0.886
	1.5	1.030	0.994	0.958	1.035	0.955	0.919	1.036	0.946	0.909
	2.0	1.039	1.022	0.940	1.044	0.988	0.935	1.046	0.974	0.921
	3.5	1.046	1.008	0.913	1.051	1.063	0.958	1.054	1.041	0.984
	5.0	1.050	1.012	0.908	1.057	1.058	0.945	1.062	1.071	0.968
	7.0	1.056	1.022	0.912	1.062	1.062	0.945	1.068	1.085	0.961
	10.0	1.058	1.016	0.951	1.067	1.070	0.941	1.072	1.094	0.959
T_4	0.5	1.026	0.896	0.872	1.029	0.900	0.872	1.028	0.901	0.872
	1.0	1.035	0.902	0.865	1.031	0.893	0.864	1.033	0.893	0.864
	1.5	1.035	0.926	0.896	1.036	0.908	0.876	1.038	0.905	0.873
	2.0	1.035	0.949	0.915	1.037	0.926	0.891	1.040	0.920	0.884
	3.5	1.039	1.013	0.973	1.046	0.980	0.932	1.048	0.970	0.921
	5.0	1.044	0.995	0.960	1.052	1.025	0.966	1.056	1.010	0.952
	7.0	1.046	0.986	0.952	1.057	1.048	1.004	1.063	1.054	0.984
	10.0	1.049	0.982	0.946	1.062	1.037	0.997	1.071	1.072	1.021

5. Method of analysis via the isolated member approach

Routine design procedures always require the development of a FE rack analysis model to evaluate internal forces and moments associated with the more representative load conditions, and, for this reason, the selection of the method of analysis via an overall exact/approximate buckling analysis does not require any additional work from designers. Furthermore, as alternatives, reverse procedures should be adopted starting from the theoretical buckling load of isolated members, before any type of structural analysis. In particular, once the geometry and the components of the rack have been defined, the value of the axial load acting on

each internal upright (N_{Ed}) can be easily evaluated by considering the transfer force mechanism. Neglecting both the presence of transversal forces (frame imperfections) and semi-rigid joints and assuming an equal uniform load on all the pallet beams, the total vertical live load on each internal upright frame (dead load in racks is generally negligible) results equal to the sum of the pallet loads acting on each load level of an internal span. As a consequence, once evaluated the elastic critical load for the isolated member, N_{cr}, the critical load multiplier α_{cr} can be simply obtained as

$$\alpha_{cr} = \frac{N_{cr}}{N_{Ed}} \tag{9}$$

where N_{Ed} (axial load on the upright) is half of the load on the upright frame.

Neglecting buckling modes due to distortional buckling phenomena, out of interest for the present paper, in case of isolated members N_{cr} is assumed as the minimum between the flexural ($N_{cr,y}$ and $N_{cr,z}$ along the principal y and z axis, respectively),the torsional ($N_{cr,T}$), and the flexural–torsional ($N_{cr,FT}$) buckling loads, which are defined on the basis of the well-established theory [16] as

$$N_{cr,F,y} = \frac{\pi^2 E I_y}{(h_{eff,y})^2} \tag{10a}$$

$$N_{cr,F,z} = \frac{\pi^2 E I_z}{(h_{eff,z})^2} \tag{10b}$$

$$N_{cr,T} = \frac{1}{i_0^2}\left[G \cdot I_t + \frac{\pi^2 E I_w}{h_{eff,T}^2}\right] \quad \text{with} \quad i_0^2 = i_z^2 + i_y^2 + y_0^2 \tag{11}$$

$$N_{cr,FT} = \frac{N_{cr,F,y}}{2\beta}\left[1 + \frac{N_{cr,T}}{N_{cr,F,y}} - \sqrt{\left(1 - \frac{N_{cr,T}}{N_{cr,F,y}}\right)^2 + 4\left(\frac{y_0}{i_0}\right)^2 \frac{N_{cr,T}}{N_{cr,F,y}}}\right]$$
$$\text{with} \quad \beta = 1 - \left(\frac{y_0}{i_0}\right)^2 \tag{12}$$

where E and G are the elastic normal and shear modulus of the material, respectively, subscripts y and z indicate the principal axes of the cross-section, h_{eff} is the effective length for flexural modes, $h_{eff,T}$ is the effective length for torsional buckling, I_t is the torsional coefficient, I_w is the warping coefficient and y_0 expresses the distance between shear center and centroid along the y axis (symmetry axis).

The most followed approach in European routine rack design is the one recommended directly by the Code, which declares that if the axial forces and bending moment in the plane of buckling of a member have been determined on the basis of a 2nd order elastic analysis, they already enhance 2nd order effects and the buckling length may be assumed equal to the system length. Furthermore, another similar clause of the code states that when 2nd order global analysis is used, it is admitted for member design to use in-plane buckling lengths for the non-sway mode. The procedure currently adopted by rack designers is to determine the non-sway elastic critical load of the rack and then, for each storey in turn, to calculate the effective length to use with the appropriate buckling curve. Due to the need to optimize the weight and hence the costs of the racks, generally the rack design is developed by selecting the cross-section of the structural members in order to guarantee a value of α_{cr} significantly lower than 10 and 2nd order analysis is hence always mandatory. As a consequence, bending moments are always increased by 2nd order effects independently on the procedures adopted for the verification checks; the elastic critical loads associated with the flexural buckling modes are evaluated in accordance with Eq. (10a) and (10b): no distinction from sway and no-sway racksis required and the effective lengths $h_{eff,z}$ and $h_{eff,y}$ are assumed equal to the height of the upright panel (h_u) and to the distance from the industrial floor to the first load level (h_{LL}), respectively. It should be noted that in order to reduce the dangerous effects associated with a incorrect evaluation of the effective length for flexural buckling in the down-aisle direction, the U.S. rack design code [8] limits the lower value of the effective length in the down-aisle direction ($h_{eff,y}$) independently of the degrees of refinement of the FE analysis tools, imposing that

$$h_{eff,y} \geq 1.7 h_{LL} \tag{13}$$

As to the effective length $h_{eff,T}(=K_T h_u)$ required to evaluate torsional buckling load, $N_{cr,T}$ (and, as a consequence, also the flexural–torsional one, $N_{cr,FT}$). European provisions recommend to use the full distance between bracing points when the connections provide full torsional restraint ($h_{eff,T}=h_u$) or half distance between bracing points when the connections provide both full torsional restraint and full warping restraint ($h_{eff,T}=0.5h_u$). In practice, being really difficult to obtain fully torsional warping restraint, $h_{eff,T}$ has been assumed in the present study equal to 0.7 times the distance between the bracing points ($h_{eff,T}=0.7h_u$), as usually it occurs in routine rack design. Buckling loads evaluated by assuming $K_T=0.5$ ($N_{cr,FT}^{K_T=0.5}$) or $K_T=1.0$ ($N_{cr,FT}^{K_T=1.0}$) are significantly different from the ones associated with $K_T=0.7$ ($N_{cr,FT}^{K_T=0.7}$).The choice of $h_{eff,T}$ is hence very important, owing to the direct influence of $N_{cr,T}$ on $N_{cr,FT}$. As an example related to M_ and T_ uprights, Fig. 12 represents the ratios $N_{cr,FT}^{K_T=1.0}/N_{cr,FT}^{K_T=0.7}$ and $N_{cr,FT}^{K_T=0.5}/N_{cr,FT}^{K_T=0.7}$ for values of effective length $h_{eff,y}$ of interest in the down-aisle direction. It can be noted

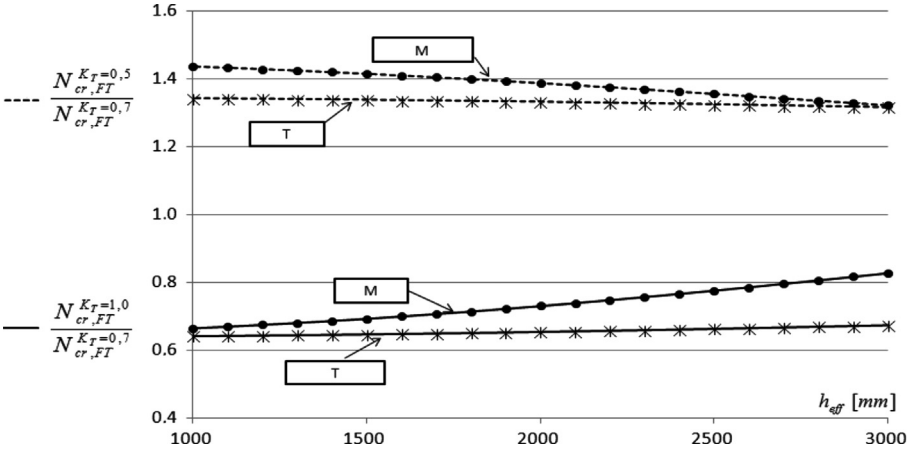

Fig. 12. Influence of effective length coefficient K_T on the flexural–torsional buckling load.

that the trends of the plotted curves are quite similar for both cross-sections. Increasing the value of the effective torsional lengths, differences from unity are reduced, more rapidly for M_racks than for T_racks. The values of the ratio are however significantly different from unity, as expected: for both the uprights, $N_{cr,FT}^{K_T=0.5}/N_{cr,FT}^{K_T=0.7}$ is always greater than 1.35 while the ratio $N_{cr,FT}^{K_T=1.0}/N_{cr,FT}^{K_T=0.7}$ ranges from 0.63 to 0.82 approximately, confirming the great importance of a correct evaluation of K_T.

A non-negligible open problem, not adequately up-to-now considered in racks design codes, is related to the evaluation of term N_{cr} for uprights belonging to semi-continuous racks unbraced, i.e. racks unbraced in the down-aisle direction with semi-rigid beam-to-column and base plate joints, providing stability to lateral forces.

The design approach based on the system length defines the flexural critical buckling load in the down-aisle direction independently on the values of the rotational stiffness of the beam-to-column joints and of the base plate connections, i.e. the same value of the flexural critical load results associated with both simple and rigidly-jointed frames. Designers could however make reference to other more appropriated alternatives providing them not in disagreement or less conservative than this one, which is the only one described in detail in the code and, for this reason, very commonly used. An efficient design option seems to be the well-established approach proposed by Wood [38] for compres-sion members in rigidly-jointed frames, suitably modified to account for the presence of semi-rigid joints. By assuming that the effective length depends directly on the restraint degrees provided by all the surrounding members, it appears often sufficient for design purposes to consider the behavior of a limited region of the frame. Furthermore, for beams not rigidly connected to the column (beams with semi-rigid end joints), the restraining end effect decreases remarkably as well as when the column is connected to the foundation via semi-rigid base plate connections. In the previous version of European standards for steel design [39], an approach based on this equivalent sub-frame model was suggested to evaluate the column effective length. In particular, with reference to Fig. 13(a), the nodal distribution stiffness coefficient η_1 and η_2, at the top and at the bottom of the column, respectively, can be defined as

$$\eta_1 = \frac{K_c + K_1}{K_c + K_1 + 1.5(K_{11} + K_{12})} \tag{14a}$$

$$\eta_2 = \frac{K_c + K_2}{K_c + K_2 + 1.5(K_{21} + K_{22})} \tag{14b}$$

where K is the stiffness coefficient given by the ratio between the second moment of area (I) and the length of the member (L), i.e. $K=I/L$, subscripts are presented in the Fig. 13 and a coefficient 1.5 takes into account the sway frame (K depending on the condition of the restrains at the opposite beam end).

In case of frames with rigid joints, the effective buckling length factor K_β required to evaluate, $h_{eff,y}$, i.e. the effective length in the down-aisle direction ($h_{eff,y}=K_\beta h_{LL}$) is defined as

$$K_\beta = \sqrt{\frac{1 - 0.2(\eta_1 + \eta_2) - 0.12\eta_1\eta_2}{1 - 0.8(\eta_1 + \eta_2) + 0.6\eta_1\eta_2}} \tag{15}$$

Furthermore, the presence of the semi-rigid connections has to be taken into account adequately by reducing suitably the stiffness coefficient K of members semi-rigidly connected to the upright. As proposed in [12], it appears necessary to use $I_{b,red}$, i.e. the reduced value of the second moment of area of the beam (I_b) having end connections with rotational stiffness $S_{j,btc}$. Reduced beam stiffness, $I_{b,red}$, can be expressed with a more satisfactory degree of accuracy as

$$I_{b,red} = I_b \frac{\varsigma}{6 + \varsigma} \tag{16a}$$

where ς is defined as

$$\varsigma = S_{j,btc} \frac{L_b}{EI_b} \tag{17a}$$

On the basis of the definitions previously introduced, it results that

$$\varsigma = S_{j,btc} \frac{L_b}{EI_b} = S_{j,btc} \frac{0.5}{S_{j,btc}^{EC3-LB}} = 0.5\rho_{j,btc} \tag{17b}$$

As a consequence, the reduced beam stiffness can be expressed:

$$I_{b,re} = I_b \frac{\rho_{j,btc}}{12 + \rho_{j,btc}} \tag{16b}$$

It should be noted that the reduction of the beam stiffness K due to the presence of the semi-rigid joints is absolutely not negligible, the reduced second moment of area ranging from 40% (if $\rho_{j,btc}=0.5$) to 83.3% (if $\rho_{j,btc}=10.0$) of one of the beams rigidly connected ($\rho_{j,btc}=\infty$).

By direct substitution, it can be immediately obtained

$$\eta_2 = \frac{2I_u L_b (12 + \rho_{j,btc})}{2I_u L_b (12 + \rho_{j,btc}) + 3I_b h \rho_{j,btc}} \tag{18}$$

In routine design of medium-rise racks the most stressed uprights are generally the ones comprised between the industrial floor and the first load level. As a consequence, also the effect of

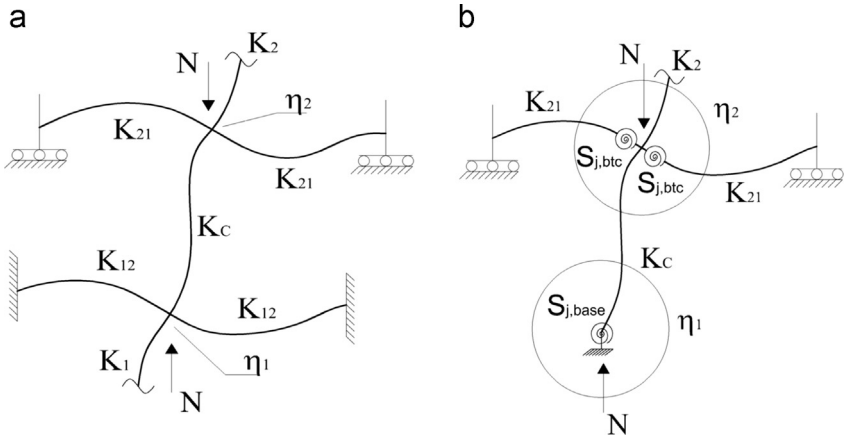

Fig. 13. Wood's equivalent frame in case of sway frame: the column of a rigidly-jointed frame (a) and the base column of a semi-continuous frame (b).

the base-plate connection reducing the degree of restraint of the bottom upright end has to be explicitly included via the end parameter η_1. The dimensionless stiffness at the bottom upright end in Eq. (14a) varies from zero (corresponding to a hinge, i.e. $\eta_1=1$) to unity (corresponding to a fixed base, i.e. $\eta_1=0$): due to the presence of the sole base-plate connection (Fig. 13b), η_1 parameter has been herein evaluated as

$$\eta_1=\frac{K_c}{K_c+S_{j,base}}=\frac{1}{1+30\rho_{j,base}} \tag{19a}$$

It should be noted that the only difference between this approach and the previous one is in the evaluation of the effective length $h_{eff,y}$: the system length is increased by term k_β. Also in this case, both torsional and flexural–torsional buckling loads have to be evaluated separately.

As further alternative, a hybrid approach should be adopted for racks with mono-symmetric cross-sections, which combines the results of a 6DOFs FE overall buckling analysis with the evaluation of the flexural–torsional buckling load of isolated members.

5.1. Numerical applications

The approaches on isolated members have been applied to the considered racks and main results are herein presented, to better individuate key features of the procedure adopted to assess the elastic critical load multiplier, α_{cr}, the following apices have been used:

- *SL* term, which is associated with the use of the system length;
- *W* term, which is associated with the use of the effective length considering the presence of semi-rigid joints via Wood's approach [38], reducing the beam stiffness as recommended by ECCS [12];
- *FT* term, which is associated with the evaluation of flexural–torsional buckling load of an isolated member;
- apex 6, which is associated with a 6DOFs FE overall buckling analysis; if all bi-symmetric cross-section members are used as rack components, α_{cr}^6 represents the exact critical load multiplier;
- apex 7, which is associated with a 7DOFs FE overall buckling analysis: multiplier α_{cr}^7 can be considered exact if racks are realized by mono-symmetric cross-section members.

In Table 5 the design alternatives of selecting the method of analysis are summarized, which are admitted, or not in contrast with the European rack provisions, and have been in the following applied on the racks described in Section 3.1. It is worth to underline the equivalence between SL and 1st superscripts and 2nd and W superscripts.

With reference to L_racks, i.e. the ones with the uprights interested only by the flexural buckling modes, Table 6 presents the ratios $\alpha_{cr}^{SL}/\alpha_{cr}^6$ and $\alpha_{cr}^{W}/\alpha_{cr}^6$. It should be noted that the approach based on the system length leads to a very unsafe (dangerous) overestimation of the elastic critical load multiplier (up to 6 times for L_3 racks and up to 10 times for L_5 racks, approximately). Increasing the stiffness of beam-to-column joints, the ratio $\alpha_{cr}^{SL}/\alpha_{cr}^6$ decreases significantly but, in any case, the lowest values are always greater than 1.5, i.e. this approach seems very inadequate for design purposes, despite the fact that is clearly recommended by European Code. With reference to the modified Wood's approach (2nd appr.), the errors decrease remarkably: maximum errors are approximately 1.7 and 2.7 for L_3 and L_5 racks, respectively and are in correspondence of the lowest value of $\rho_{j,btc}$. Increasing $\rho_{j,btc}$, the error decreases and only in case of few L_3 racks, α_{cr}^6 is slightly underestimated. Figs. 14 and 15, which are related to L_5 and L_3 racks, respectively, allow a direct appraisal of the accuracy of these approaches plotting both ratios $\alpha_{cr}^{SL}/\alpha_{cr}^6$ (solid line) and $\alpha_{cr}^{W}/\alpha_{cr}^6$ (dashed line) versus the beam-to-column stiffness joints. Influence of the column-base connection stiffness, which is absent in the 1st approach, is however very limited with reference to the 2nd one, more evident in L_5 racks rather than in L_3 racks. Figs. 16 and 17 present both the frequency and the cumulated relative frequency of ratios $\alpha_{cr}^{SL}/\alpha_{cr}^6$ and $\alpha_{cr}^{W}/\alpha_{cr}^6$, respec-tively: the former is characterized by a relevant concentration of data in the range 2–6 while the range 1–2 is of interest for the latter.

Table 6
Prediction of the buckling multiplier via the isolated member approaches considering the system length ($\alpha_{cr}^{SL}/\alpha_{cr}^6$) and the modified Wood's approach ($\alpha_{cr}^{W}/\alpha_{cr}^6$).

Racks	$\rho_{j,btc}$	$\rho_{j,base}=0.15$		$\rho_{j,base}=0.30$		$\rho_{j,base}=0.45$	
		1st *appr.* $\alpha_{cr}^{SL}/\alpha_{cr}^6$	2nd *appr.* $\alpha_{cr}^{W}/\alpha_{cr}^6$	1st *appr.* $\alpha_{cr}^{SL}/\alpha_{cr}^6$	2nd *appr.* $\alpha_{cr}^{W}/\alpha_{cr}^6$	1st *appr.* $\alpha_{cr}^{SL}/\alpha_{cr}^6$	2nd *appr.* $\alpha_{cr}^{W}/\alpha_{cr}^6$
L_3	0.5	6.039	1.724	5.672	1.712	5.551	1.709
	1.0	4.153	1.391	3.897	1.378	3.834	1.382
	1.5	3.351	1.254	3.134	1.237	3.063	1.231
	2.0	2.903	1.178	2.718	1.163	2.639	1.150
	3.5	2.268	1.072	2.087	1.040	2.030	1.030
	5.0	1.993	1.027	1.815	0.986	1.760	0.973
	7.0	1.803	0.997	1.626	0.947	1.570	0.932
	10.0	1.660	0.975	1.482	0.918	1.425	0.899
L_5	0.5	9.962	2.643	9.603	2.697	9.433	2.703
	1.0	6.568	1.981	6.330	2.017	6.248	2.030
	1.5	5.182	1.718	4.981	1.743	4.917	1.754
	2.0	4.401	1.570	4.222	1.589	4.167	1.598
	3.5	3.272	1.351	3.113	1.355	3.081	1.366
	5.0	2.767	1.248	2.627	1.249	2.580	1.249
	7.0	2.411	1.172	2.274	1.165	2.233	1.165
	10.0	2.128	1.107	1.995	1.093	1.957	1.092

Table 5
Summary of the design alternatives to evaluate buckling load multiplier via the isolated members approaches.

Appr.	Buckling mode				Load multiplier
	Flexural along		Torsional	Flexural–torsional	
	Strong axis	Weak axis			
1st	$N_{cr,Fy}$ from Eq. (10a) with $h_{eff,y}=h_{LL}$	$N_{cr,Fz}$ from Eq. (10b) with $h_{eff,z}=h_u$	$N_{cr,T}$ with $h_{eff,T}=K_T h_u$ from Eq. (11)	$N_{cr,FT}$ from Eq. (12)	$\alpha_{cr}^{1st}=\frac{\min(N_{cr,Fy},N_{cr,Fz},N_{cr,T},N_{cr,FT})}{N_{Ed}}$
2nd	$N_{cr,Fy,red}$ from Eq. (10a)) with $h_{eff,y}=K_\beta h_{LL}$ $N_{cr,Fz}$ from (10b)) with $h_{eff,z}=h_u$				$\alpha_{cr}^{2nd}=\frac{\min(N_{cr,Fy,red},N_{cr,Fz},N_{cr,T},N_{cr,FT})}{N_{Ed}}$
3rd	$N_{cr,F}=\alpha_{cr}^6\cdot N_{Ed}$ α_{cr}^6 from a buckling analysis with a 6DOFs FE beam formulation				$\alpha_{cr}^{3rd}=\min(\alpha_{cr}^6,\frac{N_{cr,T}}{N_{Ed}},\frac{N_{cr,FT}}{N_{Ed}})$
4th	$N_{cr}^7=\alpha_{cr}^7\cdot N_{Ed}$ α_{cr}^7 from a buckling analysis with a 7DOFs FE beam formulation				

K_T=torsional buckling lenght factor.
K_β=flexural buckling lenght factor.

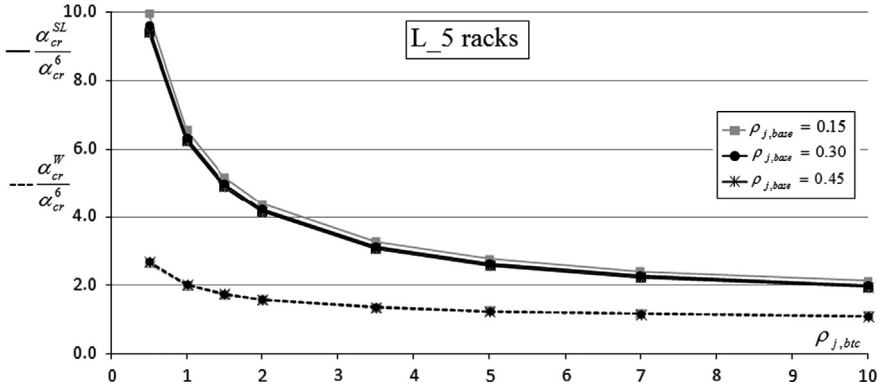

Fig. 14. Errors in the prediction of the elastic critical load multiplier, for L_5 racks.

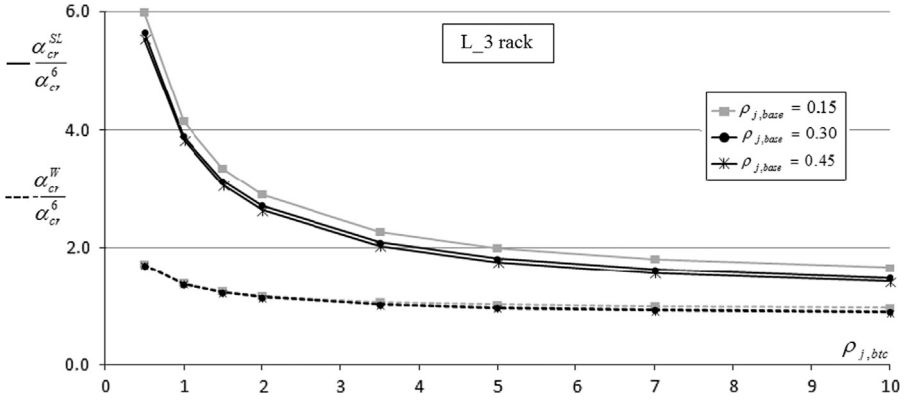

Fig. 15. Errors in the prediction of the elastic critical load multiplier, for L_3 racks.

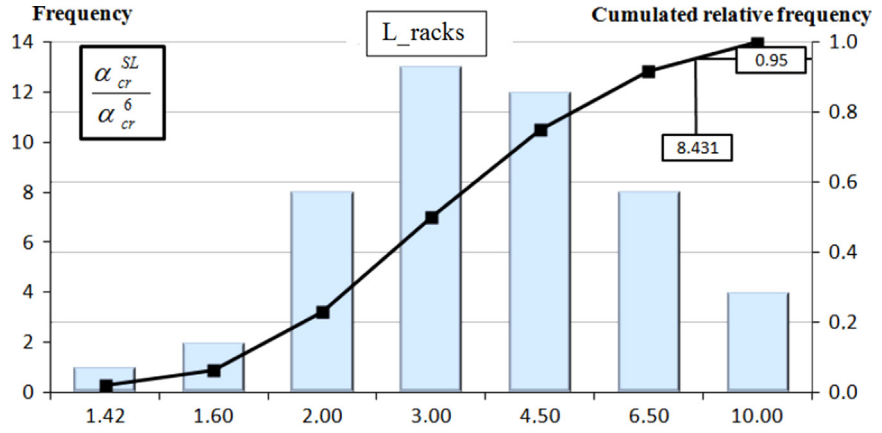

Fig. 16. Frequency and cumulated relative frequency of the ratio $\alpha_{cr}^{SL}/\alpha_{cr}^{6}$ for L_racks.

The 95% fractile value associated with the system length approach is very high, approximately equal to 8.4, significantly greater than value of 2.5 corresponding to the modified Wood's method, despite the fact that this value is however too high to recommend the application of this method in design.

If reference is made to racks composed by mono-symmetric profiles, the outcomes of the application of these approaches are summarized in Table 7, which proposes the ratios $\alpha_{cr}^{SL+FT}/\alpha_{cr}^{7}$, $\alpha_{cr}^{W+FT}/\alpha_{cr}^{7}$ and $\alpha_{cr}^{6+FT}/\alpha_{cr}^{7}$. It can be noted that:

- as for the L_racks, the worst prediction of the elastic load multiplier is associated with the system length (1st approach), but it must be remarked that the additional flexural–torsional buckling checks reduce significantly the errors. Also in this case, as it appears from Figs. 18 (M_racks) and 19 (T_racks), increasing $\rho_{j,btc}$, ratio $\alpha_{cr}^{SL+FT}/\alpha_{cr}^{7}$ decreases but with reference to $\rho_{j,btc}$=0.5 the estimated critical load multiplier is never less than 3 (M_racks) and 5 (T_racks) times the ones evaluated by buckling analysis, respectively, instead of 10 times as for

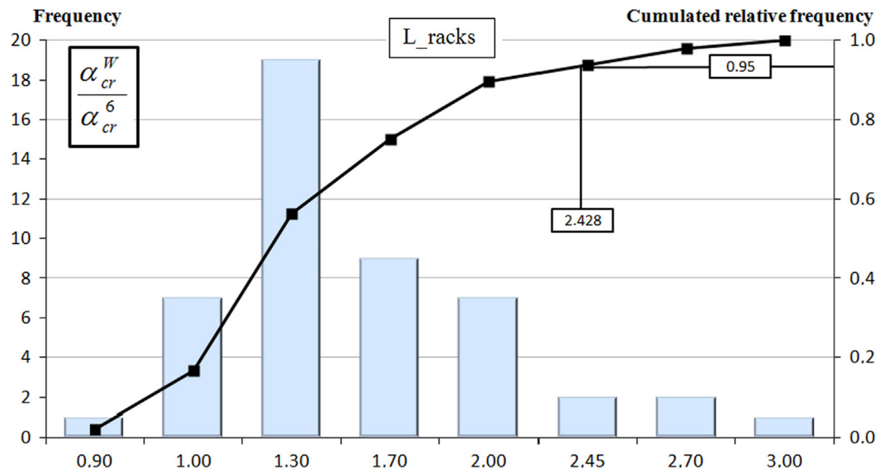

Fig. 17. Frequency and cumulated relative frequency of the ratio $\alpha_{cr}^{W}/\alpha_{cr}^{6}$ for L_racks.

Table 7
Prediction of the buckling multiplier via the isolated member approaches considering the system length ($\alpha_{cr}^{SL+FT}/\alpha_{cr}^{7}$), the modified Wood's approach ($\alpha_{cr}^{W+FT}/\alpha_{cr}^{7}$) and the hybrid approach ($\alpha_{cr}^{6+FT}/\alpha_{cr}^{7}$).

Racks	$\rho_{j,btc}$	$\rho_{j,base}=0.15$			$\rho_{j,base}=0.30$			$\rho_{j,base}=0.45$		
		1st *appr.* $\alpha_{cr}^{SL+FT}/\alpha_{cr}^{7}$	2nd *appr.* $\alpha_{cr}^{W+FT}/\alpha_{cr}^{7}$	3rd *appr.* $\alpha_{cr}^{6+FT}/\alpha_{cr}^{7}$	1st *appr.* $\alpha_{cr}^{SL+FT}/\alpha_{cr}^{7}$	2nd *appr.* $\alpha_{cr}^{W+FT}/\alpha_{cr}^{7}$	3rd *appr.* $\alpha_{cr}^{6+FT}/\alpha_{cr}^{7}$	1st *appr.* $\alpha_{cr}^{SL+FT}/\alpha_{cr}^{7}$	2nd *appr.* $\alpha_{cr}^{W+FT}/\alpha_{cr}^{7}$	3rd *appr.* $\alpha_{cr}^{6+FT}/\alpha_{cr}^{7}$
M_4	0.5	3.110	1.231	*0.927*	2.973	1.235	*0.931*	2.918	1.233	*0.924*
	1.0	2.149	1.005	*0.907*	2.038	0.997	*0.903*	2.003	0.996	*0.907*
	1.5	1.771	0.918	*0.894*	1.671	0.906	*0.889*	1.636	0.901	*0.886*
	2.0	1.571	0.874	*0.886*	1.468	0.854	*0.875*	1.441	0.851	*0.878*
	3.5	1.295	0.814	*0.862*	1.194	0.783	*0.854*	1.167	0.777	*0.855*
	5.0	1.182	0.791	*0.847*	1.079	0.754	*0.840*	1.051	0.744	*0.841*
	7.0	1.105	0.776	*0.835*	1.002	0.734	*0.829*	0.973	0.723	*0.830*
	10.0	1.048	0.767	*0.828*	0.944	0.720	*0.818*	0.914	0.707	*0.818*
M_5	0.5	3.284	1.475	*0.884*	3.169	1.487	*0.884*	3.121	1.487	*0.878*
	1.0	2.228	1.134	*0.848*	2.145	1.136	*0.844*	2.116	1.137	*0.844*
	1.5	1.812	1.001	*0.824*	1.737	0.997	*0.820*	1.713	0.997	*0.819*
	2.0	1.584	0.928	*0.806*	1.512	0.919	*0.801*	1.491	0.918	*0.800*
	3.5	1.266	0.825	*0.771*	1.203	0.812	*0.767*	1.185	0.809	*0.766*
	5.0	1.132	0.781	*0.751*	1.071	0.764	*0.747*	1.053	0.760	*0.746*
	7.0	1.040	0.751	*0.733*	0.979	0.730	*0.730*	0.963	0.726	*0.730*
	10.0	0.972	0.728	*0.717*	0.911	0.705	*0.714*	0.894	0.700	*0.715*
T_3	0.5	3.856	1.429	*0.967*	3.650	1.423	*0.972*	3.582	1.421	*0.967*
	1.0	2.686	1.161	*0.945*	2.517	1.140	*0.942*	2.465	1.135	*0.942*
	1.5	2.224	1.063	*0.930*	2.065	1.034	*0.925*	2.017	1.026	*0.924*
	2.0	1.976	1.015	*0.924*	1.825	0.981	*0.918*	1.777	0.970	*0.917*
	3.5	1.643	0.961	*0.907*	1.492	0.911	*0.897*	1.447	0.897	*0.894*
	5.0	1.508	0.946	*0.898*	1.356	0.888	*0.885*	1.310	0.870	*0.883*
	7.0	1.423	0.943	*0.892*	1.268	0.877	*0.878*	1.220	0.856	*0.874*
	10.0	1.358	0.943	*0.887*	1.203	0.871	*0.871*	1.154	0.847	*0.867*
T_4	0.5	4.896	1.747	*0.979*	4.694	1.763	*0.980*	4.617	1.765	*0.979*
	1.0	3.312	1.355	*0.965*	3.155	1.355	*0.958*	3.112	1.359	*0.959*
	1.5	2.685	1.208	*0.949*	2.547	1.201	*0.945*	2.507	1.201	*0.945*
	2.0	2.337	1.127	*0.936*	2.210	1.116	*0.932*	2.172	1.114	*0.933*
	3.5	1.862	1.023	*0.915*	1.742	1.000	*0.912*	1.705	0.994	*0.910*
	5.0	1.665	0.985	*0.904*	1.543	0.953	*0.899*	1.508	0.945	*0.898*
	7.0	1.533	0.962	*0.893*	1.409	0.922	*0.888*	1.373	0.912	*0.888*
	10.0	1.434	0.947	*0.886*	1.309	0.901	*0.879*	1.273	0.890	*0.880*

L-racks. In a very limited number of cases, this approach leads to a slight underestimation of α_{cr}^{7} but it cannot be absolutely adopted in rack design, as shown in Fig 20 where the frequency and the relative cumulated frequency of the ratio $\alpha_{cr}^{SL+FT}/\alpha_{cr}^{7}$ are plotted: the 95% fractile value is however high, being equal to 3.6, approximately;

- as it appears also from Figs. 21 and 22, related respectively to M_ and T_racks, the modfi ed Wood's approach combined with the flexural–torsional buckling checks results only in a very limited number of cases from the unsafe side (for the lowest value of $\rho_{j,btc}$); in all the other cases, the errors are significantly reduced if compared with the ones associated with system length: ratio $\alpha_{cr}^{W+FT}/\alpha_{cr}^{7}$ is never greater than 1.5 for M_ racks and 1.8 for T_ racks. From the data related to the statistical distributions plotted in Fig. 23, a relevant concentration of data can be noted in the range 0.90–1.25

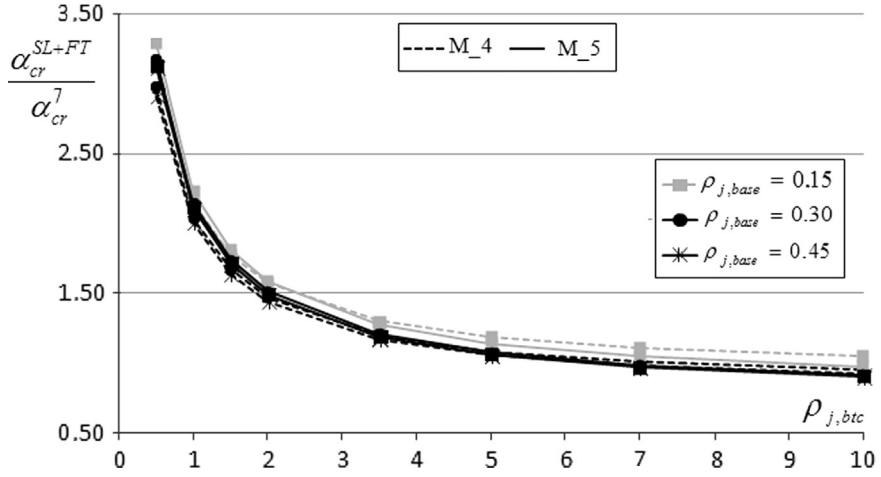

Fig. 18. Errors in the prediction of the critical load multiplier via the use of the system length for M_racks.

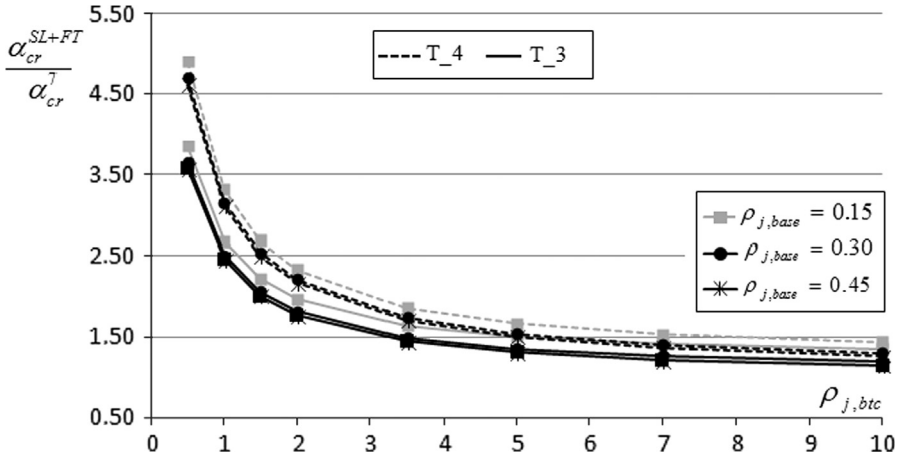

Fig. 19. Errors in the prediction of the critical load multiplier via the use of the system length for T_racks.

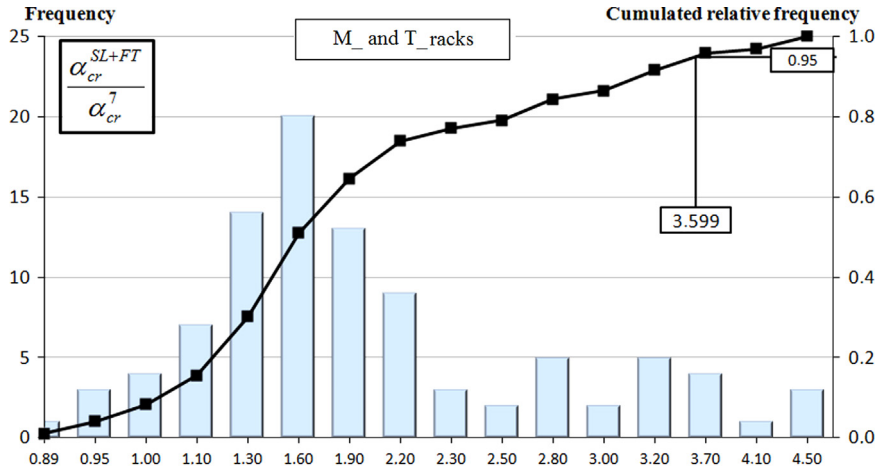

Fig. 20. Frequency and cumulated relative frequency of the ratio $\alpha_{cr}^{SL+FT}/\alpha_{cr}^{7}$ for M_ and T_ racks.

and the 95% fractile value is now reduced approximately to 1.5.

- the use of 6DOFs buckling analysis combined with the flexural–torsional checks leads to a general underestimation of α_{cr}^{7} and this approach allows the best design approximation. Errors increase with the increase of $\rho_{j,btc}$ and in the worst case (M_5 racks with $\rho_{j,base}$=0.45) they range from 0.88 to 0.71. Figs. 24 for M_racks and 25 for T_racks present the $\frac{\alpha_{cr}^{6+FT}}{\alpha_{cr}^{7}}-\rho_{j,btc}$ relationships while the frequency and cumulated relative frequency are plotted in Fig. 26. It can be noted that the 95% fractile value is equal to 0.97, approximately, confirming the adequacy of this method for design purposes.
- owing to the relevant influence of the flexural–torsional buckling on the value of α_{cr} in case of mono-symmetric uprights, more

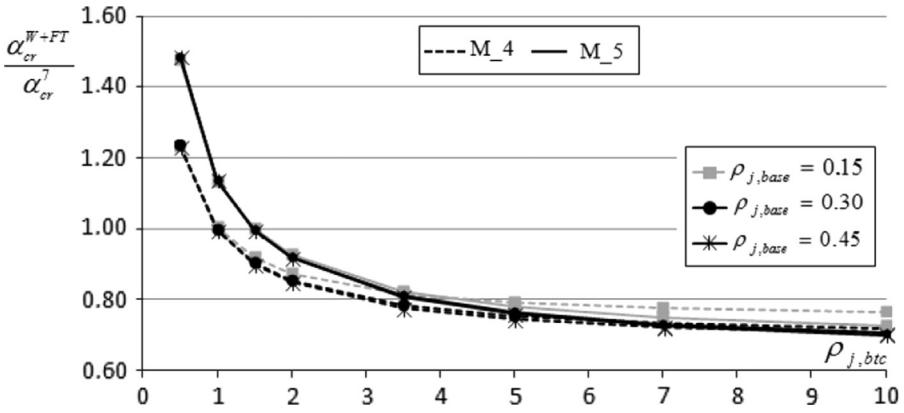

Fig. 21. Errors in the prediction of the critical load obtained via the use of the modified Wood's method for M_ racks.

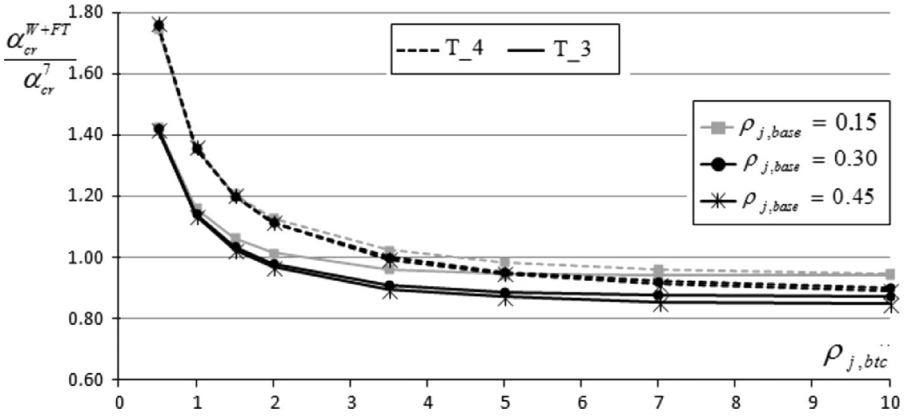

Fig. 22. Errors in the prediction of the critical load via with the use of the modified Wood's method for T_ racks.

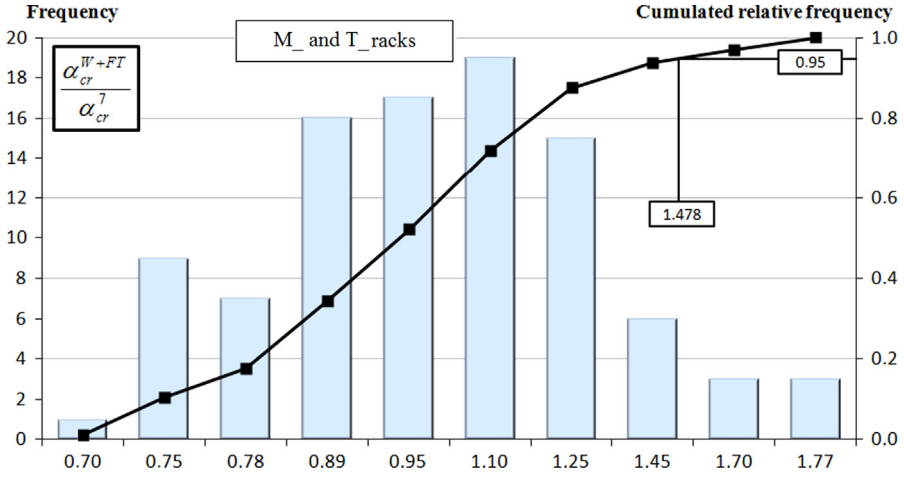

Fig. 23. Frequency and cumulated relative frequency of the errors in the critical load obtained via the modified Wood's method ($\alpha_{cr}^{W+FT}/\alpha_{cr}^{7}$) for M_ and T_ racks.

attention has been focused on the 3rd approach, recommended also by as the recently updated rack standard [9], i.e. the only approach which seems, on the basis of the Authors' experience, more than adequate for design purpose when α_{cr}^{7} cannot be directly evaluated.

In order to investigate the influence of the torsional buckling coefficient K_T, defining the effective torsional length in Eq. (11), i.e. $h_{eff,T}=K_T \cdot h_u$, Table 8 presents in addition to the ratio $\alpha_{cr}^{6+FT}/\alpha_{cr}^{7}$ obtained with K_T=0.7, already presented in Table 7 also the same ratio evaluated by considering for α_{cr}^{6+FT} the values of K_T=0.5 and K_T=1.0, identified as $\alpha_{cr}^{6+FT(K_T=0,5)}/\alpha_{cr}^{7}$ and $\alpha_{cr}^{6+FT(K_T=1,0)}/\alpha_{cr}^{7}$, respectively. It can be noted that using K_T=0.5 the accuracy in the prediction of α_{cr}^{7} increases remarkably: overestimation, of the actual critical load multiplier is never greater than 4% for T_racks and 13% for M_racks. In Fig. 27 the cumulated relative frequency of the ratios $\alpha_{cr}^{6+FT}/\alpha_{cr}^{7}$ related to K_T=0.5, K_T=0.7 and K_T=1.0 are presented together with the associated 95% fractile value, which ranges approximately from 0.91 (K_T=1.0) to unity (K_T=0.5).

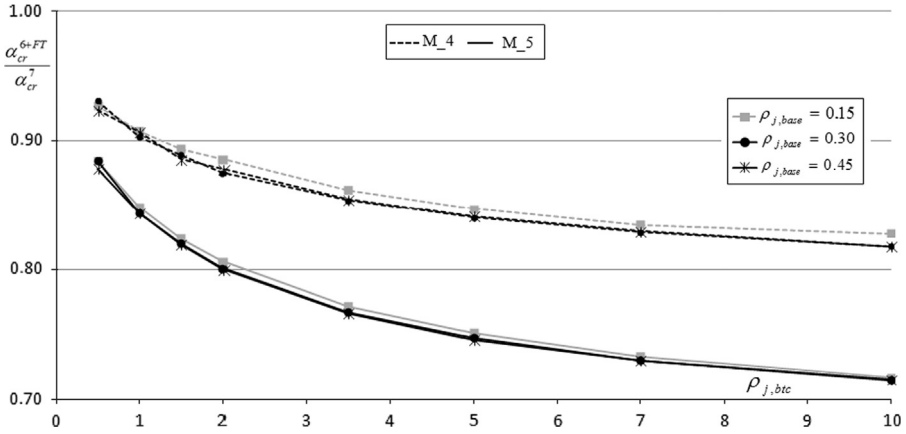

Fig. 24. Errors in the prediction of the critical load via the use of the hybrid method for the M_ racks.

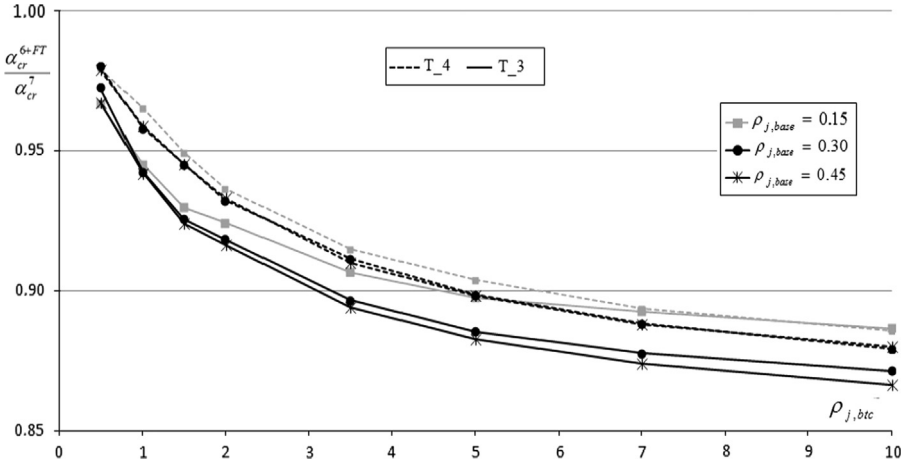

Fig. 25. Errors in the prediction of the critical load via the use of the hybrid method for the T_ racks.

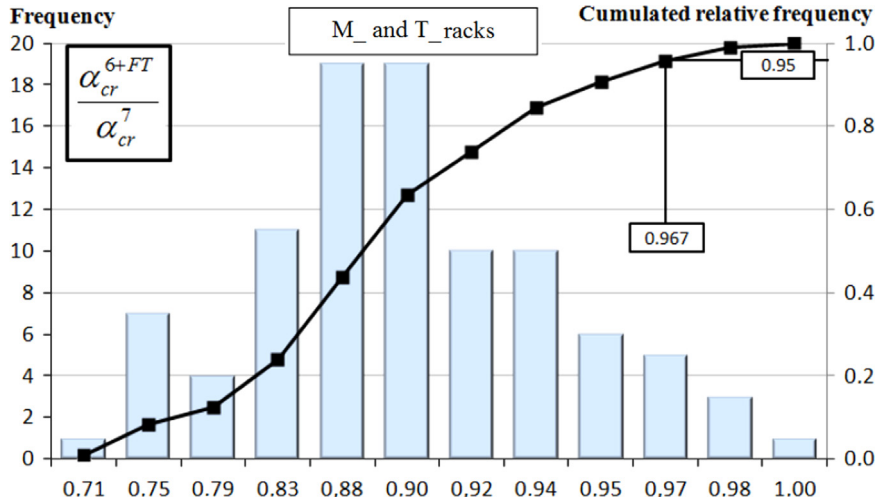

Fig. 26. Frequency and cumulated relative frequency of the errors in the critical load via the hybrid method for the M_ and T_racks.

6. Concluding remarks

Outcomes of a numerical study on the design of unbraced medium-rise pallet racks are proposed in this two-parts paper aimed at analyzing critically the approaches currently adopted for routine design in accordance with European practice. An academic FE structural analysis software has been suitably modified by Authors, which offers, in addition to the traditional 6DOFs FE beam element formulation, also the more refined 7DOFs one able to capture the complex behavior of mono-symmetric open cross-section members, which are commonly used as uprights of semi-continuous racks. As reported in the Appendix A, relevant differences can be observed for which concerns the definition of the geometric stiffness matrices, $[K]^G$. In case of traditional (6DOFs) approach, the geometric stiffness matrix $[K]^G$ of the most commonly used commercial FE analysis programs contains the sole

Table 8
Influence of the effective length factor K_T on the accuracy of the hybrid approach ($\alpha_{cr}^{6+FT}/\alpha_{cr}^{7}$).

Racks	$\rho_{j,btc}$	$\rho_{j,base}=0.15$			$\rho_{j,base}=0.30$			$\rho_{j,base}=0.45$		
		$K_T=0.5$	$K_T=0.7$	$K_T=1.0$	$K_T=0,5$	$K_T=0.7$	$K_T=1,0$	$K_T=0.5$	$K_T=0.7$	$K_T=1.0$
M_4	0.5	0.966	*0.927*	0.852	0.972	*0.931*	0.852	0.965	*0.924*	0.845
	1.0	0.963	*0.907*	0.805	0.962	*0.903*	0.797	0.967	*0.907*	0.798
	1.5	0.961	*0.894*	0.775	0.961	*0.889*	0.765	0.958	*0.886*	0.760
	2.0	0.962	*0.886*	0.755	0.955	*0.75*	0.739	0.960	*0.878*	0.739
	3.5	0.952	*0.862*	0.714	0.951	*0.854*	0.697	0.955	*0.855*	0.695
	5.0	0.943	*0.847*	0.691	0.946	*0.840*	0.674	0.951	*0.841*	0.671
	7.0	0.936	*0.835*	0.674	0.942	*0.829*	0.656	0.947	*0.830*	0.652
	10.0	0.934	*0.828*	0.662	0.936	*0.818*	0.640	0.941	*0.818*	0.635
M_5	0.5	0.940	*0.884*	0.783	0.942	*0.884*	0.779	0.937	*0.878*	0.774
	1.0	0.928	*0.848*	0.714	0.926	*0.844*	0.706	0.927	*0.844*	0.704
	1.5	0.919	*0.824*	0.670	0.920	*0.820*	0.662	0.920	*0.819*	0.660
	2.0	0.913	*0.806*	0.640	0.913	*0.801*	0.630	0.914	*0.800*	0.628
	3.5	0.900	*0.771*	0.586	0.903	*0.767*	0.576	0.904	*0.766*	0.573
	5.0	0.891	*0.751*	0.557	0.897	*0.747*	0.546	0.898	*0.746*	0.543
	7.0	0.881	*0.733*	0.534	0.889	*0.730*	0.523	0.893	*0.730*	0.520
	10.0	0.871	*0.717*	0.515	0.882	*0.714*	0.504	0.887	*0.715*	0.501
T_3	0.5	0.995	*0.967*	0.910	1.002	*0.972*	0.912	0.998	*0.967*	0.906
	1.0	0.985	*0.945*	0.865	0.985	*0.942*	0.857	0.986	*0.942*	0.854
	1.5	0.978	*0.930*	0.834	0.978	*0.925*	0.823	0.978	*0.924*	0.819
	2.0	0.980	*0.924*	0.816	0.979	*0.918*	0.802	0.979	*0.917*	0.797
	3.5	0.974	*0.907*	0.779	0.971	*0.897*	0.758	0.971	*0.894*	0.752
	5.0	0.971	*0.898*	0.760	0.967	*0.885*	0.735	0.968	*0.883*	0.728
	7.0	0.971	*0.892*	0.748	0.965	*0.878*	0.719	0.966	*0.874*	0.710
	10.0	0.968	*0.887*	0.737	0.964	*0.871*	0.706	0.964	*0.867*	0.696
T_4	0.5	1.002	*0.979*	0.933	1.004	*0.980*	0.931	1.003	*0.979*	0.929
	1.0	0.999	*0.965*	0.896	0.993	*0.958*	0.886	0.995	*0.959*	0.886
	1.5	0.991	*0.949*	0.865	0.989	*0.945*	0.856	0.990	*0.945*	0.855
	2.0	0.984	*0.936*	0.841	0.983	*0.932*	0.831	0.985	*0.933*	0.830
	3.5	0.975	*0.915*	0.797	0.976	*0.912*	0.786	0.977	*0.910*	0.782
	5.0	0.971	*0.904*	0.774	0.972	*0.899*	0.759	0.974	*0.898*	0.755
	7.0	0.967	*0.893*	0.755	0.969	*0.888*	0.738	0.972	*0.888*	0.733
	10.0	0.964	*0.886*	0.739	0.967	*0.879*	0.720	0.971	*0.880*	0.715

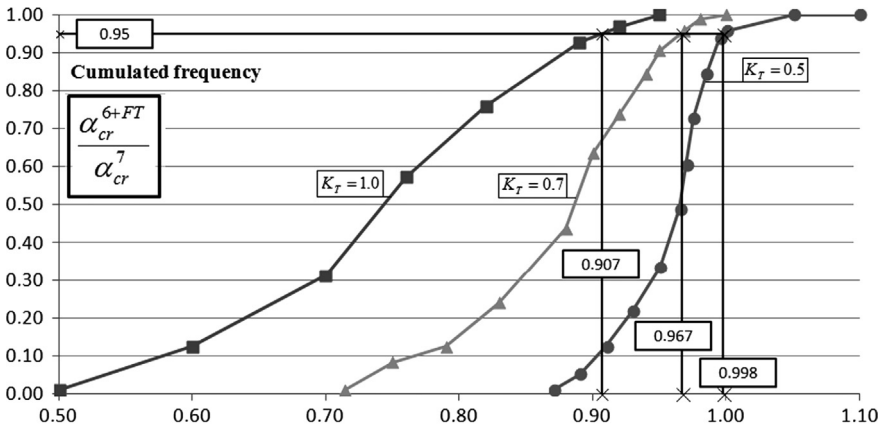

Fig. 27. Cumulated relative frequency of the errors in the critical load via the hybrid method with ($K_T=0.5$,$K_T=0.7$ and $K_T=1.0$) for the M_ and T_ racks.

value of the axial force while by considering all the warping effects (7DOFs) this matrix depends also strictly on the values of internal forces, bending and torsional moments. The parameters of the numerical study on racks have been selected in order to propose a general overview related to cases commonly encountered in rack design practice. Furthermore, the case of rack formed by uprights with a double-symmetric cross-section has been considered, too.

In the present part of this two-parts paper, attention has been focused on the selection of the method of analysis, which represents the initial phase of each design process and, in case of racks, it is of primary importance, due to the direct and non negligible influence of 2nd order effects on displacements, internal forces and moments: this choice depends on the sole value of the critical load multiplier and, hence, the different alternatives admitted by the European design code have been discussed and applied to the considered racks. It should be noted that:

- if overall buckling analysis is used in case of bi-symmetrical uprights (L_racks), the obtained results indicate that bending moment distributions don't influence the elastic critical load of racks and hence the traditional 6DOFs formulations accounting for the presence of the sole axial load in the geometric stiffness matrix seem adequate for practical design purposes. The use of the Horne's method allows to predict from the safe side the

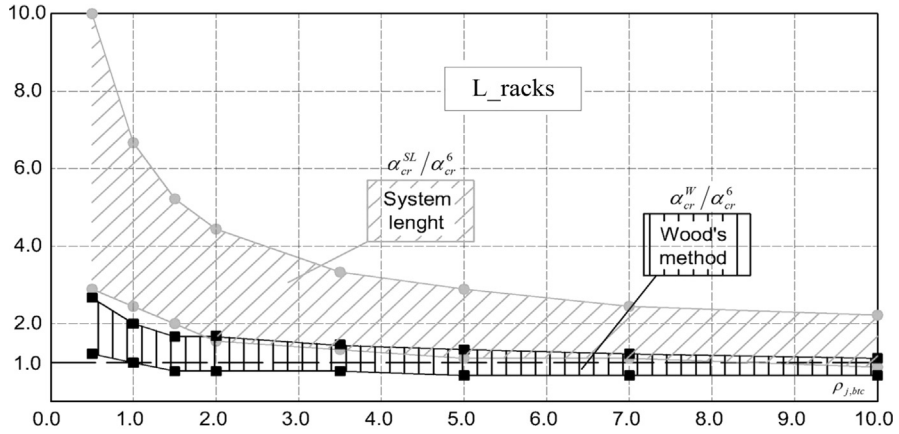

Fig. 28. Domain of errors of the predicted critical load via the modified Wood's method or the system length for the L_racks.

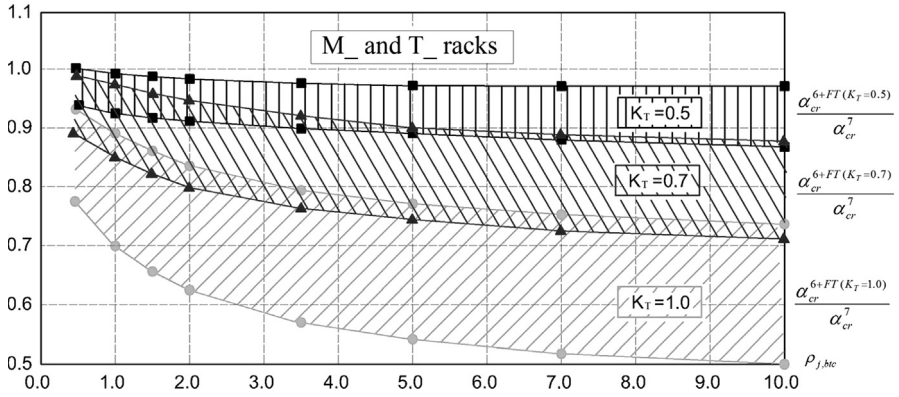

Fig. 29. Influence of the effective length factor (K_T) on the errors accuracy of the prediction of the critical load via the hybrid method.

critical load multiplier quite accurately, especially for higher values of the joint stiffness. With reference to the isolated member approaches, both the system length and the modified Wood's approach have been discussed and applied; the accuracy of both methods can be appraised via Fig. 28, where their domains are reported: it can be observed that, despite the greater accuracy of the modified Wood's approach, errors are however too elevate for design purposes;

- in case of mono-symmetric cross-section members, the absence of warping effects in the overall buckling analysis leads to over-estimate significantly the elastic critical load multiplier, up to 16%, leading consequently to an un-conservative choice of the method of analysis. Furthermore, the use of the approximate Horne's method should be recommended only if the set of 7DOFs displacements is available; otherwise it can lead to an over-estimation of the overall buckling load. As to the selection via the isolated member approach it has been shown that the weak point of the European rack code requirements [6] regards the evaluation of the flexural buckling load in the down-aisle direction. As clearly shown, the provisions allow to evaluate flexural buckling load multiplier on the basis of the system length and this choice (1st approach), which is commonly followed in routine design, leads to a great over-estimation of the values of load associated with critical load condition. It has been demonstrated that contrarily to what explicitly declared by the European code, this approach is greatly unsafe: lower errors can be obtained via the 2nd approach (based on Wood's studies). Finally, the hybrid alternative (3rd approach), i.e. the buckling 6DOFs analysis combined with the flexural–torsional buckling on members, allows to assess the critical load multiplier from the safe side and with more limited errors: it appears the only approach adequate for design purposes. Particular care should be paid to the assessment of effective length factor K_T, which, as it results from the domains presented in Fig. 29, influences significantly the accuracy of the method and could lead to estimate also very accurately α_{cr}^{7}, if adequate restraints to torsional buckling are provided.

As a general conclusion, the discussed research outcomes demonstrate that these further improvements of the European rack code are urgently expected for the safe evaluation of the flexural buckling load of isolated members. Furthermore, clear and univocal requirements for the selection of the method of analysis are urgently expected, too, owing to the absolutely non negligible influence of warping effects when mono-symmetric cross-section uprights are used.

Appendix A. On the stiffness matrix for a 7DOFs FE beam formulation

For members having mono-symmetric cross-section, finite element (FE) beam formulations are significantly different if compared with the ones adopted for bi-symmetric cross-sections. With reference to Fig. 3, let us denote j and k the two nodes of the generic beam, the governing matrix displacement equations of the FE element can be written in a general form [17–19], for both elastic $[K]^E$ and geometric $[K]^G$ stiffness matrices, such as:

$$\left[\begin{array}{c|c} [K]_{jj} & [K]_{jk} \\ \hline [K]_{kj} & [K]_{kk} \end{array}\right] \left[\begin{array}{c} \{u\}_j \\ \hline \{u\}_k \end{array}\right] = \left[\begin{array}{c} \{f\}_j \\ \hline \{f\}_k \end{array}\right] \tag{A1}$$

With reference to the more general case of 7DOFs beam formulation, the nodal displacement, $\{u\}_j$ and $\{u\}_k$, and the

associated force vectors, $\{f\}_j$ and $\{f\}_k$, can be defined respectively as

$$\{u\}_j = \begin{bmatrix} u_o \\ v_s \\ w_s \\ \varphi_x \\ \varphi_y \\ \varphi_z \\ \{\theta\} \end{bmatrix} \tag{A2a}$$

$$\{f\}_j = \begin{bmatrix} N \\ F_y \\ F_z \\ M_t \\ M_y \\ M_z \\ \{B\} \end{bmatrix} \tag{A2b}$$

The presence of terms θ (warping) and B (bi-moment) occurs only in the FE beam formulations include the 7th DOF. These formulations are very complex, especially for what concerns the definition of the geometric stiffness matrix $[K]^G$, as clearly stated in Ref. [22].

With reference to a beam element of length L, considering its area (A), second moments of area along principal axes (I_z and I_y), de Saint Venant's torsional and warping constants (I_t and I_w, respectively) and assuming E and G representing Young's and tangential material modulus, respectively, the stiffness elastic

The terms between curly brackets are related to the sole formulations including warping effects, by means of the 7th DOF (θ), which influences directly also the term associated with uniform torsion, i.e. term 4.4. It should be noted that the classical 6DOFs beam formulations are characterized, for which concerns the elastic stiffness matrix, $[K]^E$, by the presence of term GI_t/L, while in the 7DOFs formulation the contribution $\left\{\frac{12EI_w}{L^3}+\frac{1}{5}\frac{GI_t}{L}\right\}$ has to be directly added (for $[K]^E_{jj}$) in sub-matrix (A3a)) or subtracted (for $[K]^E_{jj}$) in sub-matrix (A3b)) to GI_t/L.

Furthermore, with reference to the geometric stiffness matrix, $[K]^G$, the traditional 6DOFs beam formulations implemented in several commercial FE analysis software [18,32] require the dependence on the sole value of the internal axial load N. Otherwise, in case of beam formulations including warping, also bending moments (M_y and M_z), torsional moment (M_t), bi-moment (B) and shear actions (F_y and F_z) contribute significantly to the geometric stiffness, $[K]^G$, the terms that depend strictly also on the distance between the load application point and shear center.

Let's focus the attention on the geometric stiffness associated with a mono-symmetric cross-section, if the axis of symmetry is the y axis, therefore $z_0=0$, as for the cross-sections considered in the present paper (Fig. 4). The complete and exhaustive definition of $[K]^G$ is not herein presented because of its length, being however out of interest for the goal of the present paper. Reference can be made in literature [21–24]. In the following, the parameters of the cross-section k_{ij} are reported in sub-matrix $[K]^G_{jj}$ by means of their dependence on internal forces and moments.

$$[K]^G_{jj} = \left[\begin{array}{cccccc|c} k_{11}(N) & 0 & 0 & 0 & 0 & 0 & 0 \\ & k_{22}(N) & 0 & \{k_{24}(M_y)\} & \{k_{25}(M_t, M_y y_0)\} & k_{26}(N) & \{k_{27}(M_y)\} \\ & & k_{33}(N) & \{k_{34}(N y_0 M_z)\} & k_{35}(N) & \{k_{36}(M_t, M_y y_0)\} & \{k_{37}(N y_0 M_z)\} \\ & & & k_{44}(N\alpha_x, \{M_z\alpha_z, B_\omega\alpha_\omega\}) & \{k_{45}(N y_0, M_z)\} & \{k_{46}(M_y)\} & \{k_{47}(N\alpha_x, M_z\alpha_z, B_\omega\alpha_\omega)\} \\ & & & & k_{55}(N) & 0 & \{k_{57}(N y_0 M_z)\} \\ & & & \textit{symmetric} & & k_{66}(N, \{M_z y_0\}) & \{k_{67}(M_y)\} \\ \hline & & & & & & \{k_{77}(N\alpha_x, M_z\alpha_z, B_\omega\alpha_\omega)\} \end{array}\right] \tag{A4}$$

sub-matrices $[K]^E_{jj}$ (or, equivalently, $[K]^E_{kk}$) and $[K]^E_{jk}$ (or $[K]^E_{kj}$) are defined as

$$[K]^E_{jj} = \left[\begin{array}{cccccc|c} \frac{EA}{L} & 0 & 0 & 0 & 0 & 0 & 0 \\ & \frac{12EI_z}{L^3} & 0 & 0 & 0 & \frac{6EI_z}{L^2} & 0 \\ & & \frac{12EI_y}{L^3} & 0 & -\frac{6EI_y}{L^2} & 0 & 0 \\ & & & \frac{GI_t}{L}+\left\{\frac{12EI_w}{L^3}+\frac{1}{5}\frac{GI_t}{L}\right\} & 0 & 0 & \left\{\frac{6EI_w}{L_3}+\frac{3}{30}\frac{GI_t}{L}\right\} \\ & & \textit{Symmetric} & & \frac{4EI_y}{L} & 0 & 0 \\ & & & & & \frac{4EI_z}{L} & 0 \\ \hline & & & & & & \left\{\frac{4EI_w}{L_3}+\frac{4}{30}\frac{GI_t}{L}\right\} \end{array}\right] \tag{A3a}$$

$$[K]^E_{jk} = \left[\begin{array}{cccccc|c} -\frac{EA}{L} & 0 & 0 & 0 & 0 & 0 & 0 \\ 0 & -\frac{12EI_z}{L^3} & 0 & 0 & 0 & \frac{6EI_z}{L^2} & 0 \\ 0 & 0 & -\frac{12EI_y}{L^3} & 0 & -\frac{6EI_y}{L^2} & 0 & 0 \\ 0 & 0 & 0 & -\frac{GI_t}{L}-\left\{\frac{12EI_w}{L^3}+\frac{1}{5}\frac{GI_t}{L}\right\} & 0 & 0 & \left\{\frac{6EI_w}{L^3}+\frac{3}{30}\frac{GI_t}{L}\right\} \\ 0 & 0 & \frac{6EI_y}{L^2} & 0 & \frac{2EI_y}{L} & 0 & 0 \\ 0 & -\frac{6EI_z}{L^2} & 0 & 0 & 0 & \frac{2EI_z}{L} & 0 \\ \hline 0 & 0 & 0 & \left\{-\frac{6EI_w}{L^3}-\frac{3}{30}\frac{GI_t}{L}\right\} & 0 & 0 & \left\{\frac{2EI_w}{L^3}-\frac{1}{30}\frac{GI_t}{L}\right\} \end{array}\right] \tag{A3b}$$

In this case, the terms between curly brackets are related to the sole formulations including the 7th DOF (warping). Term y_0 represents the eccentricity between the shear center and the centroid of the cross-section, while terms α_i are Wagner's coefficients defined as

$$\alpha_x = \frac{I_z + I_y}{A} + y_0^2 \tag{A5a}$$

$$\alpha_z = \frac{1}{I_z}\left(\int_A y^3 dA + \int_A z^2 y dA\right) - 2y_0 \tag{A5b}$$

$$\alpha_\omega = \frac{1}{I_\omega}\left(\int_A \omega z^2 dA + \int_A \omega y^2 dA\right) \tag{A5c}$$

where the terms in expression represent the area (A), the second moments of area (I_z and I_y) along principal axes and the warping constants.

It should be noted that the 7DOFs FE beam formulation includes the 6DOFs one. This can be easily obtained disgracing the 7th DOF in case of the cross-section having two axis of symmetry (i.e. $y_0=0$, $\alpha_z=\alpha_\omega=0$). As a consequence, the geometric stiffness sub-matrix, obtained by eliminating warping terms is

reduced to the form presented in Eq. (A6).

$$[K]_{ij}^{G}=\begin{bmatrix} k_{11}(N) & 0 & 0 & 0 & 0 & 0 \\ & k_{22}(N) & 0 & \{k_{24}(M_y)\} & \{k_{25}(M_t)\} & k_{26}(N) \\ & & k_{33}(N) & \{k_{34}(M_z)\} & k_{35}(N) & \{k_{36}(M_t)\} \\ & & & k_{44}(N\alpha_x) & \{k_{45}(M_z)\} & \{k_{46}(M_y)\} \\ & \textit{symmetric} & & & & \\ & & & & k_{55}(N) & 0 \\ & & & & & k_{66}(N) \end{bmatrix} \tag{A6}$$

Furthermore, it should be noted that the terms contributing to define the geometric stiffness are bending moments (M_y and M_z), torsional moment (M_t), and the Wagner's constant α_x in addition to the axial load N.

Finally, it should be noted that, with reference to the most common 6DOFs commercial FE programs, geometric stiffness matrix contains only the value of axial loads, i.e. the terms between the brackets in sub-matrix (A6) are absent.

Appendix B. List of symbols

Latin lower case letters

$\overline{n}$ = non-dimensional axial load.
$\overline{m}$ = non-dimensional bending moment.
h = height.
k = term of matrix, length factor.
u = displacement along the x axis.
v = displacement along the y axis.
w = displacement along the z axis.
x = longitudinal axis of the beam.
y = symmetry axis of the cross-section.
z = non symmetry axis of the cross-section.

Latin upper case letters

A = *cross-section area.*
B = bi-moment.
DOF = degrees of freedom.
E = Young's modulus.
F = shear force.
FE = finite element.
G = shear modulus.
H = height.
I = second moment of area.
K = stiffness matrix, stiffness coefficient, effective length factor.
L = length.
M = moment.
N = axial force.
S = beam-to-column joint stiffness, base-plate joint stiffness, first moment of area (section modulus).

Greek lower case letters

$\overline{\phi}$ = non-dimensional joint rotation.
α = load multiplier, Wagner's coefficients.
β = dimensionless eccentricity.
ϕ = out-of-plumb.
γ = safety factor.
η = nodal distribution stiffness coefficient.
φ = rotation.
θ = warping function.
ρ = radius gyrator of inertia, non-dimensional rotation stiffness.
ω = sectorial area.
ζ = non-dimensional rotation stiffness.

Subscripts

b = beam.
base = base-plate connection.
btc = beam-to-column connection.
cr = critical.
Ed = design value.
eff = effective.
F = flexural buckling.
FT = flexural–torsional buckling.
j = end node of the beam element, joint.
k = end node of the beam element.
LL = load level.
max = maximum.
o = position of the centroid.
pl = plastic
Rd = resistance value.
red = reduced.
s = position of the shear center, sway index.
t = torsion.
T = torsional buckling.
u = upright.
w = warping.
x = longitudinal axis of beam element.
y = symmetry axis of the cross-section, yielding of the material.
z = non symmetry axis of the cross-section.
ω = sectorial area.

Superscripts

6+FT = 6DOFs FE analysis combined with the flexural–torsional buckling.
6 = FE analysis with a beam element formulation having 6DOFs per node.
7 = FE analysis with a beam element formulation having 7DOFs per node.
E = elastic stiffness matrix.
EC3-LB = Eurocode lower bound of the semi-rigid domain.
EC3-UB = Eurocode upper bound of the semi-rigid domain.
FT = Flexural torsion.
G = geometric stiffness matrix, global resistance check.
H = Horne's method.
KT = torsional buckling coefficient.
SL = system length.
SL+FT = system length combined with the flexural–torsional buckling.
W+FT = Wood's method combined with the flexural–torsional buckling.
W = Wood's method

References

[1] Shafer BW. Cold-formed steel structures around the world – a review of recent advances in applications, analysis and design. Steel Constr 2011;4:141–9.
[2] Dubina D, Ungureanu V, Landolfo R. ECCS eurocode design manual. Oxford: Wiley-Blackweel and Ernest&Sohn; 2013.
[3] Godley MHR. Storage racking. In: Rhodes, editor. Design of cold formed steel members. London, UK: Elsevier Applied Science; 1991. p. 361–99 (chapter 11).
[4] Takeuchi T, Suzuki K. Performance-based design for truss-frame structures using energy dissipation devices. In: Mazzolan FM, editor. Proceedings of the STESSA; 2003. p. 55–61.
[5] Baldassino N, Zandonini R. Design by testing of industrial racks. Adv Steel Constr 2011;7(1):27–47.
[6] CEN, EN 15512. Steel static storage systems – adjustable pallet racking systems – principles for structural design. CEN European Committee for Standardization; 2009. p. 137.

[7] Federation Européenne de Manutention, FEM 10.2.08-Reccomendations for the design of static steel storage pallet racks in seismic conditions, version 1.00; September 2010.
[8] RMI, MH 161 specification for the design, testing and utilization of industrial steel storage racks. RMI – Rack Manufacturers Institute; 2008. p. 59.
[9] Australian Standards, AS 4084 – Steel Storage Racking, AS Standards, Australia; 2012.
[10] Bernuzzi C, Gobetti A, Gabbianelli G, Simoncelli M. Śiva-system of incremental and vibration analysis: software for a finite element analysis for beam with warping influence; 2014 [in preparation].
[11] Bathe KJ, Wilson EL, Iding RH. NONSAP-finite element calculation for non-linear static and dynamic analysis of complex structures. Berkeley, California, USA: Structural Engineering Laboratory, University of California; 1978.
[12] ECCS-European Convention for Structural Steelworks. Analysis and design of steel frames with semi-rigid joints. Publication no. 67; 1992.
[13] Baldassino N, Bernuzzi C. Analysis and behaviour of steel storage pallet racks. Thin walled Struct 2000;37(4):277–304.
[14] Dinis PB, Young B, Camotin D. "Local-distortional interaction in cold-formed steel rack-section column". Thin Walled Struct 2014;81:185–94.
[15] Vlasov VZ. Thin walled elastic beams. 2nd ed. Jerusalem: Israel Program for Scientific Transactions; 1961.
[16] Timoshenko SP, Gere JM. Theory of elastic stability. 2nd ed. New-York: McGraw Hill; 1961.
[17] Bathe K, Wilson EL. Numerical methods in finite element analysis. Englewood Cliffs: Prentice-Hall; 1976.
[18] Werkle H. Finite element in der Baustatik. Braunschweig-Wiesbaden: Vieweg; 2008.
[19] Zienkiewicz OC, Taylor RL. The finite element method. Oxford: Butterworth Heinemann; 2000.
[20] Bernuzzi C, Pieri A, Squadrito V. Warping influence on the static design of unbraced steel storage pallet racks. Thin-Walled Struct 2014;79:71–82.
[21] Bernuzzi C, Gobetti A, Gabbianelli G, Simoncelli M. Warping influence on the resistance of uprights in steel storage pallet racks. J Constr Steel Res 2014;101:224–41.
[22] Chen WF, Atsuta T. Theory of beam-columns. Space behaviour and design, 2. J. Ross Publishing; 2008.
[23] Turkalj G, Brnic J, Prpic-Orsic J. Large rotation analysis of elastic thin walled beam-type structures using ESA approach. Comput Struct 2003;81:1851–64.
[24] Battini, JM. Co-rotational beam elements in instability problems. Technical Report from Royal Institute of Technology Department of Mechanics: Stockholm, Sweden; January 2002.
[25] ConSteel 7.0: Finite-Element-Program. Consteel Solutions Ltd., ⟨http://www.consteel.hu⟩.
[26] ABAQUS/STANDARD User's Manual Version 6.8. Hibbit, Karlsson and Sorensen, USA; 2006.
[27] LS-DYNA, ⟨http://www.ls-dyna.com/1_pages/1lsdyna.htm⟩.
[28] The SOFiSTiK FEM Packages, ⟨http://www.sofistik.com/en/⟩.
[29] European Committee for Standardization CEN, Eurocode 3 – Design of Steel Structures – Part-1: General Rules and Rules for Buildings. CEN European Committee for Standardization.
[30] European Committee for Standardization CEN, Eurocode 3 – Design of Steel Structures – Part-8: Design of Steel Joints. CEN European Committee for Standardization.
[31] Filiatrault A, Higgins PS, Wanitkortkul A. Experimental stiffness and seismic response of pallet-type steel storage rack connectors. Pract Period Struct Des Constr, ASCE 2006;11:161–70.
[32] Wilson EL. Three-dimensional static and dynamic analysis of structures. Berkeley: CSI Inc.; 2002.
[33] McGuire W. Computer-aided analysis. In: Dowling PJ, Harding JE, Bjorhovde R, editors. Costructional steel design – an international guide. New York: Elsevier Applied Science; 1992. p. 915–31.
[34] Teh LH, Clarke MJ. Co-rotational and Lagrangian formulations for elastic three-dimensional beam finite elements. J Constr Steel Res 1998;48:123–44.
[35] Teh LH. Cubic beam elements in practical analysis and design of steel frames. Eng Struct 2001;23:1243–55.
[36] Teh LH, Hancock GJ, Clarke MJ. Analysis and design of double sided high-rise steel pallet rack frames. J Struct Eng 2004;130:1011–21.
[37] Horne MR. An approximate method for calculating the elastic critical loads of multi-storey plane frame. Struct Eng 1975;53(6):242–8.
[38] Wood RH. Effective lengths of columns in multi-story buildings-part 1 effective lengths of single columns and allowance for continuity. Struct Eng July 1974;52:235–44.
[39] CEN, ENV 1993-1-1 Eurocode 3 Design of Steel Structures: Part 1-1 General Rules and Rules for Buildings. CEN European Committee for Standardization.